Applied Petrological Services

PETROLOGICAL STUDIES
OF
SUB-SURFACE SAMPLES
FROM TAMAMI GOLD DEPOSITS/PROSPECTS:

METAMORPHISM AND METASOMATISM OF GOLD MINERALISATION AND IMPLICATIONS FOR EXPLORATION

FOR
NEWMONT AUSTRALIA LTD

January 2005

APS Report 257
Project No. 26005

Main Road
St Arnaud
New Zealand

Telephone (64) (3) 5211 034
Facsimile (64) (3) 5211 030
anthony@aps.co.nz

SUMMARY

1. New petrological data of this study derived from samples taken from the Callie, DBS, Windy Hill, Bunkers, Quorn and Groundrush deposits compare favourably with previously compiled petrological data from other Tanami prospects/deposits, these including Old Pirate, Hyperion, Titania and Western Tanami deposits/prospects (Coyote etc). The favourable comparison supports a model involving thermal metamorphic and related metasomatic overprinting of lode gold deposits hosted by a range of low-grade regional metamorphic rock types. Amongst the petrological data there is evidence for local and potentially more extensive remobilisation of gold protore in association with the processes thermal and metasomatic overprinting. Beyond the thermal metamorphic effects that are causative to metasomatism and ore remobilisation, there is potential for the primary mineralisation to be genetically related to granitoid intrusions. While there is potential for this style of mineralisation to be genetically related to granitoid intrusions, it is petrologically distinct from the essentially unequivocal Intrusion Related class of gold mineralisation defined at Twin Bonanza.

2. Common to many of the variably thermally and metasomatically class of lode gold deposits in the Tanami is a significant bismuth component to metallic gold chemistry. In some examples this coincides with significant whole rock bismuth chemistry and in some the bismuth bearing gold is intimately associated with complex bismuth-telluride-sulphide minerals. Whether the bismuth content of gold is significant in the absence of associated bismuth whole rock geochemistry or complex bismuth mineralogy requires further investigation. Reviews of the Intrusion-Related class of gold deposit reveal a gold-bismuth association as part of the classification criteria and with this and other criteria the Twin Bonanza prospect complies. Further work is required in order to ascertain whether or not the gold-bismuth associations, of varying extent and nature, evident in the class of metamorphosed/metasomatised lode gold deposits have any relevance in terms of Intrusion Related gold classification.

3. The chemistry of metasomatic/metamorphic biotite in gold bearing quartz veins of the metamorphosed/metasomatised class of gold deposit reveals variable fluorine enrichment. From the available relevant literature on fluorine enrichment in biotite in relation to fluorine activity in hydrothermal fluids, the fluorine enrichment in biotite is indicative of an igneous hydrothermal influence. In the examples of thermally metamorphosed/metasomatised gold systems in the Tanami, such an igneous hydrothermal influence could have taken place during primary quartz vein formation or during subsequent thermal metamorphic overprinting. In the example of the latter, magmatic volatile fluid flow may have been combined with the mainly locally generated metasomatic fluid flow. The variation in fluorine enrichment in biotite analyses of this study is consistent with the possibility of both early and late magmatic influences.

4. The genetic models of mineralisation as discussed in this report have been reviewed in terms of applications to gold exploration in the Tanami. These applications include aspects of alteration, a gold “nugget” effect and ore upgrade, host rock types, metamorphic grade, metallurgy and igneous association.

5. Ultimately this report identifies petrological applications including specialised lithoteque database establishment, early prospect characterisation, a review of the application of gold and bismuth geochemistry, a review of applications of biotite chemistry, application of xenotime/monazite dating, metasomatic fluid flow modeling, petrological interpretation of geophysical data and hydrocarbon petrology.

INTRODUCTION

In recent APS reports, interpretations of petrological data have conveyed the concept of thermal and genetically related metasomatic overprinting of protore gold mineralisation. These include studies of rocks from Old Pirate (26023), Hyperion (26022) and Lamaque/Oberon-Titania (26023). These studies find that there is petrological evidence for thermal metamorphic overprinting of hydrothermally altered and mineralised regionally metamorphosed rocks. Consistent with this concept, gold related hydrothermal activity might have significantly pre-dated the emplacement of voluminous igneous intrusion(s) causative to the thermal metamorphic overprinting.

In the example of Hyperion (26022), it was considered that rates of conductive heat transfer from cooling igneous plutons into surrounding rock will have limited the time-frame for gold mineralising hydrothermal systems that were post-igneous emplacement to around 300,000 to 800,000 years. This time-frame limitation has significance to genetic modeling of gold deposits where possible magmatic fluid sources may be invoked, or structural influences of igneous intrusion geometry are to be considered. Interpretations of petrological data from Old Pirate (26023) include that gold minerals, mainly electrum, have been locally mobilised within the confines of metamorphosed vein assemblages hosted by both metamorphosed sedimentary and igneous rocks. As a result of these processes gold minerals are also localised within metamorphosed sulphide-bearing hydrothermal wallrock replacement assemblages. The extent of gold and other element mobilisation beyond the microscopic scale is not yet fully determined.

The concept of thermal metamorphic and related metasomatic overprinting of early hydrothermal mineralisation has also been attended to in an APS Power-Point presentation which expands upon the significance of two petrologically distinct types of quartz (± carbonate and other minerals) veining found in the Tanami Region (26015). In a final version of this presentation it is ultimately concluded that a "type A" veining represents thermal and metasomatic overprinting of "type B" veining, but that "type B" veining may also locally post date "type A" veining in association with retrograde metamorphic and hydrothermal events. The Power-Point presentation (26015) also gave attention to the implications of timing of gold mineralisation and emplacement of intrusions causative to thermal overprinting, and the variable degree or grade of thermal overprinting depending on proximity of gold mineralisation to causative intrusions. In the Tanami, while there is what might be considered unequivocal Intrusion-Related gold mineralisation in the form of granitoid hosted gold deposits such as that at Twin Bonanza and Galifrey, a genetic relationship between intrusions and variably metamorphosed gold deposits located peripheral to intrusions, remains equivocal.

This report serves mainly to compile more petrological evidence for thermal and metasomatic overprinting of gold mineralised veining and hydrothermal alteration from analysis of rock samples from Callie, DBS, Groundrush, Quorn, Bunkers and Windy Hill Deposits. This study will also evaluate and re-interpret petrological data from the Western Tanami (Coyote, Pebbles etc) made available to Newmont through due diligence processes. Following recommendations outlined in the 26015 presentation, this current study will also look at the fluorine content of biotite and distribution of bismuth in gold as possible paragenetic indicators of gold mineralisation in the variably thermally metamorphosed and metasomatised deposits. As a means of comparison, electron microprobe analyses have been obtained from gold grains in the Twin Bonanza deposit.

Petrographic/mineragraphic descriptions of samples from the Callie, Groundrush, Bunkers, Quorn, Windy Hill and DBS deposits are presented in Appendix One, whereas gold, sulphide and biotite chemistry is presented in Appendix Two and Three.

RESULTS

PETROGRAPHY/MINERAGRAPHY: METAMORPHOSED AND METASOMATISED GOLD BEARING QUARTZ VEINS

Bunkers and Quorn: Rock Types (primary lithologies and replacement), veining and mineralisation

TABLE ONE. PETROGRAPHIC/MINERAGRAPHIC SUMMARY: BUNKERS AND QUORN

Sample	Comment	Lithology and Replacement	Deposition
26005.01 Bunkers ore zone	Native gold is associated with the dominant metamorphic wallrock replacement assemblage. Thermal metamorphism and metasomatism were apparently synchronous, or metamorphism post-dated metasomatism.	Laminated mudstone and siltstone (calcareous) -amphibole, biotite, orthopyroxene, muscovite, clinopyroxene, quartz, spinel, pyrite, pyrrhotite, garnet -clays (after orthopyroxene), hematite (after spinel ??)	1. (vein/cement) quartz, amphibole, clinopyroxene, biotite, muscovite, orthopyroxene, opaques, pyrite, pyrrhotite, gold
26005.1b Bunkers ore zone	Minerals common to quartz vein assemblages and wallrock replacement, including amphibole, pyrrhotite and clinopyroxene, suggest hydrothermal fluids were in equilibrium with wallrock or had been simultaneously thermally overprinted.	Laminated mudstone and siltstone -clinopyroxene, amphibole, biotite, garnet, muscovite, plagioclase, quartz, muscovite, pyrite, rutile, pyrrhotite -clay minerals (smectite, kaolinite)	-(veinlet/vein) quartz, biotite, amphibole, clinopyroxene, pyrrhotite, chalcopyrite, pyrite, chalcopyrite (→ chalcocite)
26005.2a Quorn ore zone	The metamorphic replacement assemblage comprising amphibole, clinopyroxene and orthopyroxene is best interpreted in terms of proximal thermal metamorphism; i.e. pyroxene hornfels.	Laminated/bedded sediment -clinopyroxene, amphibole, orthopyroxene, sphene, ilmenite -hematite, hydrated Fe-oxides	-(vein/cement) quartz, amphibole, clinopyroxene, sphene, ilmenite, As-pyrite, pyrrhotite -(veinlet) hematite, clay minerals
26005.2b Quorn ore zone	Biotite and green-blue amphibole are common to the metamorphic replacement assemblage and quartz vein assemblages. Saline fluid inclusions are present.	Interbedded mudstone and silty mudstone -amphibole, biotite, sphene, ilmenite, rutile, garnet, pyrrhotite and pyrite	-(vein/cement) quartz, amphibole, molybdenite ?, pyrrhotite; carbonate

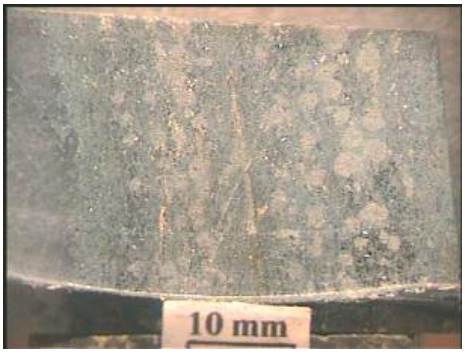

Left. 25005.2b. Bedding/lamination structure preserved by secondary mineralogy including garnet.
Right. 25005.1a. Garnet concentrated after possible primary carbonate laminae or early hydrothermal carbonate.

Peak metamorphic replacement of wallrock comprises assemblages of pyroxene (orthopyroxene and clinopyroxene) + amphibole (blue-green) + biotite + muscovite + quartz ± garnet ± pyrite ± pyrrhotite ± plagioclase ± sphene ± rutile ± spinel. Weathering assemblages comprising hematite, hydrated Fe-oxides and smectite/kaolin clays have formed after the peak metamorphic replacement assemblages. The distribution of the mainly granoblastic peak metamorphic replacement assemblages preserves a primary lamination or bedding structure. The distribution and concentration of garnet within some planar structures in particular appears to highlight a primary lamination structure (particularly as observed in hand-specimen). The planar concentrations of garnet partly defining lamination structures are parallel to quartz veining and as part of a thermal metamorphic replacement assemblage may be representative of the distribution of early hydrothermal carbonate minerals formed preferentially after (calcium-bearing) sedimentary laminae.

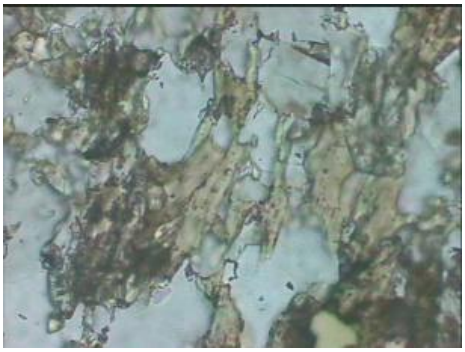

Left. 26005.01. Vein assemblage comprising interlocking quartz, amphibole and biotite. 300 μm. ppl.
Right. 26005.02. Gas-filled/rich and aqueous liquid-rich inclusions in quartz. 120 μm. ppl.

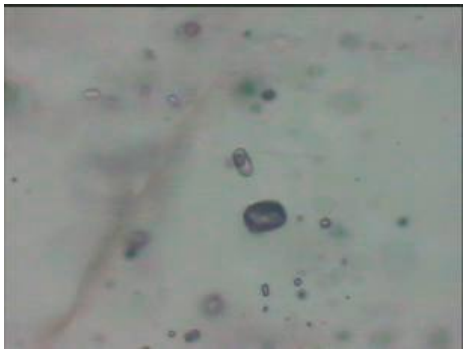

The vein assemblages are dominated by granoblastic quartz interlocking with less abundant (fluorine-bearing) hornblende, clinopyroxene, muscovite, orthopyroxene, and (fluorine-rich) biotite mainly at vein-wallrock margins. Textures indicate that an early quartz vein assemblage has been metamorphosed together with the wallrock lithology, in which calc-silicate minerals and biotite at wallrock margins may be representative of metamorphic overprinting of a hydrothermal alteration assemblage genetically related to the pre-metamorphic quartz vein assemblage.

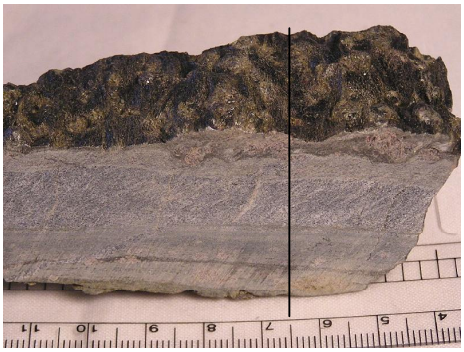

Left. 26005.02. Garnet rich bands in metasediment hosting metamorphosed quartz vein.
Right. 26005.02 section. Multiple bands of garnet rich metamorphic replacement assemblages proximal to quartz vein.

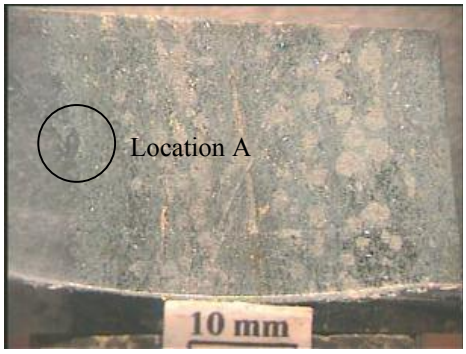

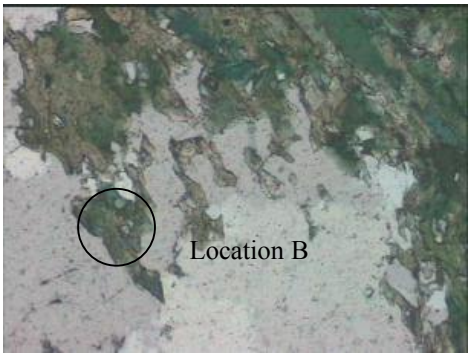

Left. 26005.02. Location A. Vein-wallrock interface, with quartz interlocking with amphibole. 1200 μm. ppl.
Right. 26005.01. Location B. Gold inclusion in hornblende at vein-wallrock margin. 120 μm. rl.

Subtle deformation fabrics, including low-wavelength crenulation folding, represented within the wallrock replacement assemblages translate into the vein assemblage and the overall evidence is that a thermal overprint and related strain post-date quartz veining. Relict primary, pseudosecondary or secondary fluid inclusions contained within the granoblastic quartz comprising populations of gas-rich inclusion types co-existing with aqueous liquid-rich inclusion types represent localised metasomatism associated with the thermal/metamorphic overprint rather than fluids from which the primary vein assemblage was formed. Relict gold grains are enclosed by hornblende after early hydrothermal mineralogy at vein-wallrock margins.

Callie : Rock Types (primary lithologies and replacement), Veining and Mineralisation

TABLE 2. PETROGRAPHIC/MINERAGRAPHIC SUMMARY: CALLIE			
26005.03 Magpie schist ore zone	The quartz veining fractures preferentially along the stringers of alkali feldspar thus exposing gold on fracture surfaces. Galena occupies the same paragenetic position as gold (inclusions in K-spar).	Siltstone/mudstone -chlorite, biotite, muscovite, rutile, ilmenite, pyrite, apatite -chlorite	-(vein) quartz, alkali feldspar (albite and orthoclase), biotite (→chlorite), muscovite (→ illitic clay, carbonate), apatite, native gold, rutile, pyrrhotite, pyrite, sphalerite, galena, chalcopyrite; carbonate -(veinlet) carbonate, pyrite
26005.04 Magpie schist ore zone	Biotite is concentrated at wallrock margins. Carbonate is interstitial to quartz and as late secondary fluid inclusions within quartz. Early and late chlorite is present.	Silty mudstone/mudstone -quartz, chlorite, biotite, muscovite, rutile, ilmenite -chlorite	-(vein) quartz, K-feldspar, Albite, biotite, muscovite, apatite; pyrrhotite, rutile, sphalerite, chalcopyrite, galena; carbonate -(veinlet) carbonate
26005.05	A metamorphosed mudstone wallrock as evidenced by the abundance of muscovite, chlorite and biotite. Carbonate is widely interstitial to quartz in the vein assemblage and overprinting feldspar and muscovite.	?sedimentary rock -muscovite, chlorite, quartz, biotite, quartz, rutile, ilmenite -chlorite	-(vein) quartz, K-feldspar (→carbonate), albite, biotite (→chlorite), muscovite, apatite, xenotime, rutile, pyrrhotite; carbonate -(veinlet) carbonate
26005.06 Ore zone, Lower Blake beds	Gold occurs as intergrowths with brown biotite, alkali feldspar (→ carbonate and illite) and quartz close to the vein-wallrock interface. Gold occurs with gas-rich/filled inclusions.	Laminated silty mudstone -chlorite, biotite, quartz, muscovite, rutile, ilmenite, pyrite/As-pyrite -chlorite	-(vein) quartz, alkali feldspar (→ illite, carbonate), biotite (→ chlorite), apatite, xenotime; rutile, pyrite/As-pyrite, chalcopyrite, gold, galena -(veinlet) carbonate

Samples from the Callie deposit represent thermal metamorphic overprinting of gold-bearing quartz veined meta-sedimentary rocks within a subtle strain environment. Within the wallrock assemblages, matrices comprising fine-grained muscovite and chlorite dispersed with courser grained brown (Ti-rich) biotite and aggregates of biotite represent thermal overprinting of regionally metamorphosed pelitic rocks. Some amounts of retrograde chlorite are present.

Left. 26005.06. Meta-mudstone (host to mineralised quartz veining) with strain fabric evident.
Right. 26005.06. Biotite plates intergrown with fine-grained muscovite after mudstone. Sub-preferred orientation of mica minerals defines a strain fabric. Ppl. 600 μm.

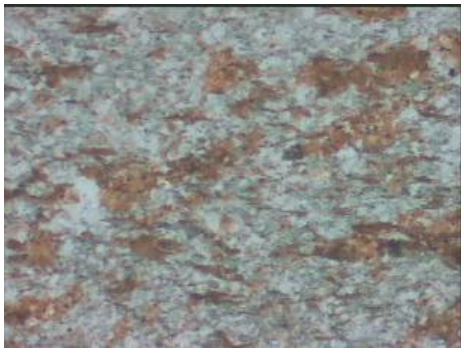

The metamorphosed veining and vein assemblages have been deformed together with the wallrock at elevated temperatures with monoclinal folding of veins and semi ductile deformation generally evident. Strain fabrics within the wallrock defined partly by peak metamorphic biotite propagate into vein assemblages. While some of the strain fabrics within the wallrock, defined mainly by recrystallised muscovite within the matrix, may pre-date veining, strain fabrics associated with peak-metamorphic replacement mineralogy, post-date primary vein formation.

Left. 26005.03. Metamorphosed quartz veined meta-mudstone.
Right. 26005.03. Sectioned meta-quartz vein. Alkali feldspar and muscovite (white domains) interposed with quartz (grey areas) define "ghosted" boudinage structures in the veins.

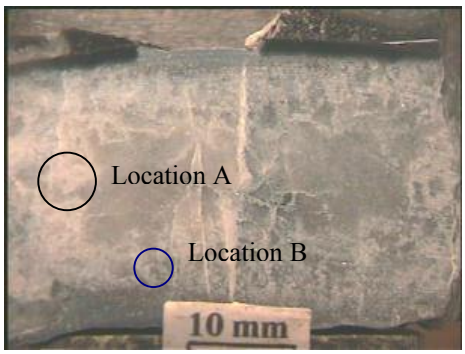

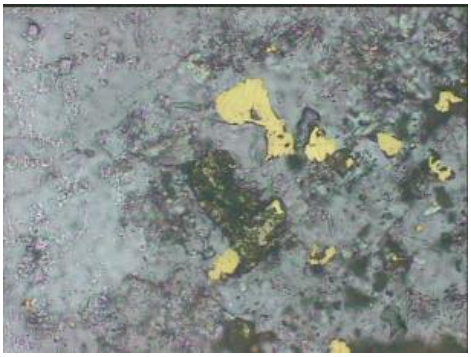

Left. 26005.03. Location A. Native gold intergrown with pyrrhotite, K-feldspar, muscovite and quartz. 300 μm. rl/ppl.
Right. 26005.03. Location B. Intergrowths of quartz, muscovite, K-feldspar and biotite within the quartz vein at wallrock margin. 300 μm. rl/ppl.

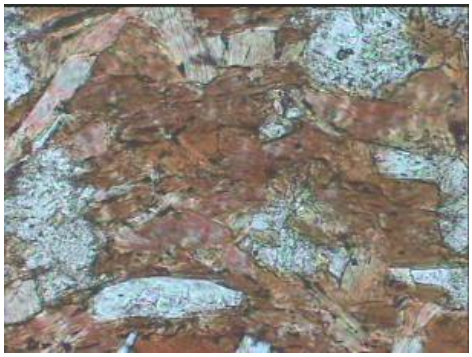

The vein assemblages comprise recrystallised quartz interlocking with platy biotite, muscovite and alkali feldspar together with minor amounts of other minerals including apatite, rutile, carbonate, pyrrhotite, pyrite, xenotime and base metal sulphides. The vein textures, including recrystallised quartz but more significantly the crystalline nature of biotite, muscovite and alkali feldspar, are more consistent with metamorphic replacement assemblages than those precipitated directly from hydrothermal fluids: The assemblages best represent metamorphic recrystallisation or replacement of mineralogy precipitated from hydrothermal solutions. This interpretation is consistent with continuity observed between peak metamorphic biotite in the wallrock with that present in the vein assemblages. Biotite in the wallrock and vein margins may in part be representative of metamorphism of sericite + chlorite ± carbonate hydrothermal assemblages primarily associated with the early vein assemblage.

Left. 26005.04. Plastically deformed and thermally overprinted, quartz vein and host mudstone.
Right. 26005.04. Section through thermally overprinted and deformed quartz vein.

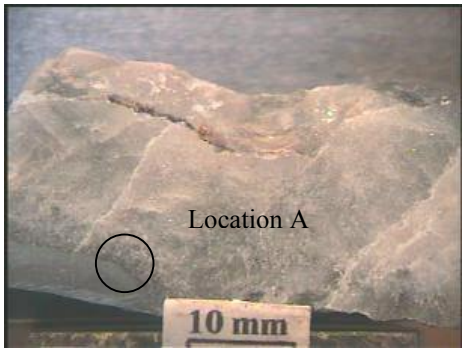

Left. 26005.04. Location A. Biotite with chlorite + muscovite replacement at quartz vein margin. Strain and thermal overprint to both wallrock and quartz vein. ppl. 1200 μm.
Right. 26005.04. Galena interstitial to and as inclusions in recrystallised quartz. Ppl/rl. 120 μm.

Secondary fluid inclusions, of complex composition (CO_2-bearing/rich co-existing with aqueous liquid-rich types) contained mainly along annealed microshears within the recrystallised quartz are interpreted to represent metasomatic fluids associated with peak thermal metamorphism (of vein and wallrock). In some places these inclusions co-exist with base metal sulphides inclusions (galena, sphalerite and chalcopyrite), these inclusion trails also linking with anhedral base metal sulphides contained interstitially to recrystallised quartz.

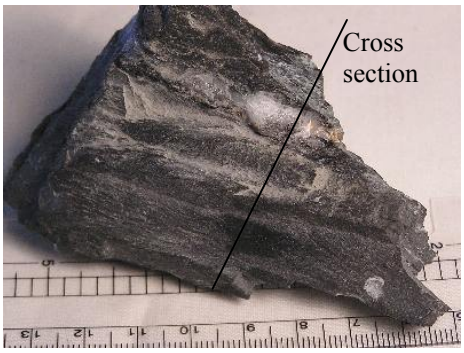

Left. 26005.06. Metamorphosed quartz veined mudstone.

Right. 26005.06. Section through metamorphosed wallrock and quartz vein.

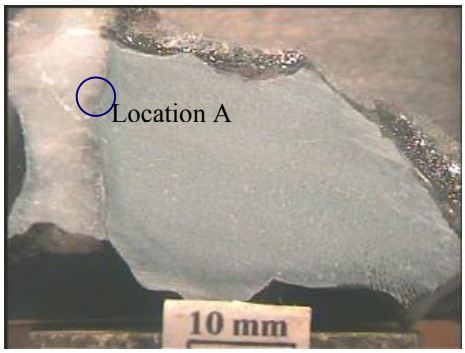

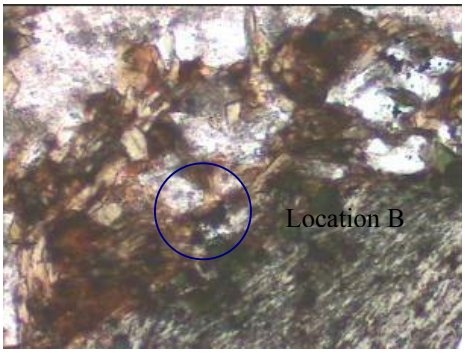

Left. 26005.06. Location A. Crystalline quartz + biotite + K-feldspar assemblage in quartz vein at wallrock margin. 1200 μm. ppl.
Right. 26005.06. Location B. Native gold intergrown with biotite and K-feldspar.

Gold identified in the vein assemblages occurs as inclusions within or intergrowths with metamorphic biotite, alkali feldspar, muscovite and quartz. Gold intergrown with or as inclusions

within biotite mostly coincides with vein-wallrock margins, where the biotite bearing assemblages represent replacement of hydrothermal assemblages with which the gold was primarily precipitated. A feature of the metamorphosed quartz veins of this study is the occurrence of gold as intergrowths with alkali feldspar, the distribution of which defines "ghosted" boudinage fabrics/structures within the metamorphosed quartz veins. As well as being located along vein-wallrock margins, alkali feldspar is concentrated at regular intervals as narrow, diffuse bands spanning the width of the veins (linking opposing wallrock margins). The veins break preferentially along these bands of concentrated alkali feldspar, and because this is a locus of gold, these fracture surfaces typically expose abundant visible gold. As part of metamorphic replacement assemblages, the concentrations of alkali feldspar are likely to represent former silicate minerals (probably including sericite) that were concentrated within dilational structures formed at high angles to vein margins during attenuation of the primary vein assemblages. Gold (and other elements) was probably remobilised to these dilational sites during secondary (metasomatic) fluid flow and primarily intergrown with hydrothermal mineralogy prior to ultimate peak metamorphic replacement (and recrystallisation of quartz).

Windy Hill: Rock Types (primary lithologies and replacement), Veining and Mineralisation

TABLE 3. PETROGRAPHIC/MINERAGRAPHIC SUMMARY: WINDY HILL			
26005.07 Windy Hill ore zone	The primary quartz vein assemblage, comprising mostly quartz, is recrystallised, resulting in the granoblastic texture now preserved. The aggregates of very fine to ultra fine-grained amphibole are part of the recrystallisation assemblage.	Sedimentary rock -quartz, muscovite, biotite, Al-silicates/feldspars -Fe-oxides, hematite, clays	-(vein) quartz, apatite, amphibole, rutile, pyrrhotite, ?base metal sulphides -(veinlet/cavity) hematite, hydrated Fe-oxides
26005.08 Windy Hill ore zone	The granoblastic vein quartz plus inclusions is representative of recrystallisation of primary quartz + silicate + sulphide vein assemblage. The abundant biotite, muscovite, pyrrhotite, rutile, amphibole and tourmaline inclusions are part of that recrystallisation assemblage.	Laminated sedimentary rock -quartz, biotite, muscovite, ?feldspar/Al-silicates -smectite/kaolin clays, hydrated Fe-oxides	-(vein) quartz, muscovite, biotite, pyrrhotite, pyrite, rutile, ?sulphides -(veinlet/cavity) hydrated Fe-oxides and hematite

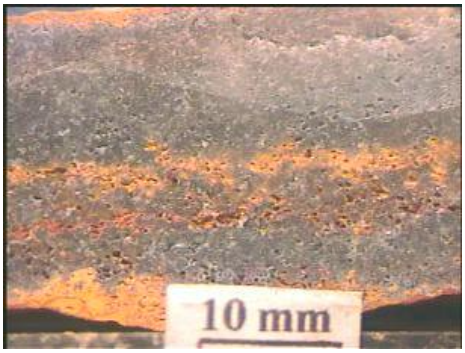

Left. 26005.07. Vitreous, smoky grey, quartz vein material.

Right. 26005.07. Green amphibole interlocking with granoblastic textured quartz. 600 μm. ppl.

Metamorphic replacement textures and mineralogy are preserved in mineralised quartz vein and adjacent wallrock material from an oxidised zone within the Windy Hill open pit. While gold mineralogy is not identified and sulphide mineralogy is poorly preserved within the oxidised

environment, the nature of a peak metamorphic replacement assemblage is resolvable. The vein assemblages dominated by quartz have been recrystallised in conjunction with peak metamorphic replacement of the wallrock lithologies. Granoblastic quartz vein textures are continuous with granoblastic textured peak metamorphic replacement textures within the metamorphosed sedimentary wallrock. Ghosted Al-silicate minerals comprise part of the peak metamorphic wallrock replacement assemblages. Hornblende is a very minor part of the granoblastic vein assemblage, and ghosted and partly preserved base metal sulphides and pyrrhotite occur as inclusions within and interstitial to quartz and hornblende.

Groundrush: Rock Types (primary lithologies and replacement), Veining and Mineralisation

TABLE 4. PETROGRAPHIC/MINERAGRAPHIC SUMMARY: GROUNDRUSH			
26005.09 Ground-rush ore zone	There is a strong gold association with K-feldspar + biotite + amphibole + Ti-oxide metasomatism within the wallrock. A gold quartz vein association is also present.	Quartz bearing dolerite -amphibole, albite/plagioclase, rutile, ilmenite, sphene, native gold -biotite, amphibole, K-feldspar, rutile, native gold, chalcopyrite, arsentiferous pyrite; carbonate -chlorite, sericite/illite, carbonate	-(cement/vein) quartz, amphibole (→ carbonate), biotite (→ chlorite) K-feldspar, pyrite, arsentiferous pyrite, native gold, chalcopyrite; carbonate -(veinlet) carbonate, pyrite

In sample material from the Groundrush open-pit ore zone, native gold is intergrown with and as inclusions within crystalline intergrowths of alkali feldspar, amphibole (actinolite), biotite and chlorite which form part of a thermal metamorphic overprint to a hydrothermal breccia cement enclosing fragments of metamorphosed mafic igneous rock. The cement assemblage comprises recrystallised, granoblastic to porphyroclastic textured quartz interlocking with grains of relatively coarse-grained platy biotite and chlorite and less abundant K-feldspar and amphibole.

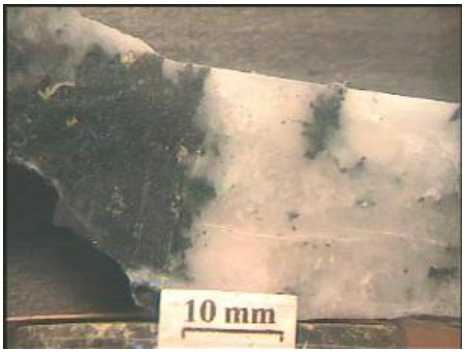

Left. 26005.09a. Thermally overprinted and plastically deformed quartz vein and dolerite wallrock. Right. 26005.09a. Wallrock -vein margin. Biotite interlocking with porphyroclastic textured quartz. Biotite is intergrown with amphibole. 600 μm. ppl.

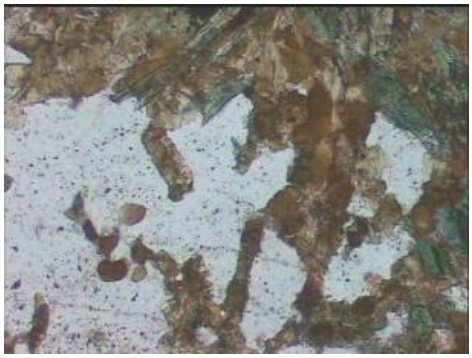

Native gold is mostly associated with metamorphic replacement of wallrock material enclosed by the thermally overprinted quartz cement. Compositionally complex fluid inclusions in the recrystallised quartz represent metasomatic fluids associated with the peak metamorphic overprint.

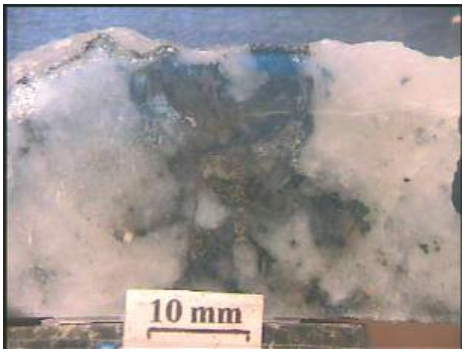

Left. 26005.09b. Thermally overprinted and deformed quartz vein breccia enclosing mafic wallrock material. Right. 26005.09b. Native gold intergrown with K-feldspar, amphibole and biotite. 600 μm. rl/ppl.

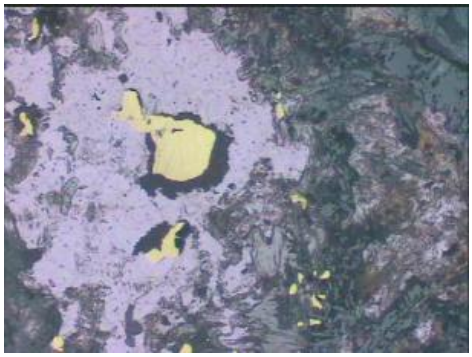

GOLD GRAIN CHEMISTRY

TABLE 5. GOLD GRAIN CHEMISTRY (SUMMARISED FROM APPENDIX 2)

Paragenesis	Analysis	Au wt%	Ag wt%	Bi wt%	TOTAL
Lower Blake Beds, underground exposure (26005). Gold intergrown with biotite, K-feldspar and quartz at wallrock-vein margins. Bismuth bearing galena is interstitial to recrystallised quartz.	6.1 a	94.01	6.54	0.53	101.24
	6.1 b	91.73	7.27	0.58	100.11
	6.1 c	92.39	6.43	0.71	99.96
Magpie schist, underground exposure (26005). Gold intergrown with K-feldspar at "boudin-necks" in close spatial association with bismuth-bearing galena, quartz and pyrrhotite.	3.3a	90.98	8.46	0.64	100.12
	3.3b	90.52	8.78	0.45	99.79
Groundrush, pit floor (26005). Gold as inclusions in and intergrown with K-feldspar, biotite and quartz after wallrock fragment in a thermally overprinted quartz + carbonate + mica vein assemblage.	9.1a	92.68	6.54	0.54	99.83
	9.1b	92.84	6.39	0.97	100.27
	9.1c	93.18	6.95	0.59	100.81
	9.1d	92.84	6.16	0.60	99.94
	9.1e	93.16	6.46	0.67	100.42
DBS gold ore (26005, DBD352/197.8). Gold as inclusions in and interstitial to recrystallised quartz in close spatial association with arsenopyrite, biotite and pyrrhotite.	dbs.1a	69.73	14.23	0.80	84.81
	dbs.2b	75.82	13.72	0.73	90.40
Hyperion, diamond core (26002). Gold intergrown with native bismuth, bismuth tellurides, bismuth tellurium sulphides, and platinum bearing iron-bismuth sulphides in recrystallised quartz vein assemblage.	8.1a	85.19	13.64	0.89	100.54
	8.1h	82.68	16.41	0.71	99.99
	8.2b	81.04	15.49	0.67	97.36
Titania, diamond core (26003). Gold inclusions in quartz, carbonate and as intergrowths with pyrite and arsenopyrite in metamorphosed quartz + carbonate + sulphide veins. Galena is locally present in the carbonate minerals.	1b.1	96.81	4.58	0.71	102.18
	1b.2	95.40	3.93	0.61	101.22
	1b.3	97.90	4.28	1.20	103.68
	1b.4	95.37	3.97	0.39	100.71
	1b.5	95.73	4.57	0.70	101.16
	1b.6	95.20	4.55	0.79	102.67
	1b.8	97.55	4.88	1.09	104.15
	1b.9	96.18	4.30	0.78	101.42
	1b.12	96.47	4.58	1.03	102.17
Twin Bonanza (26021). Gold as inclusions in arsenopyrite in igneous hydrothermal breccia.	21-3a1	85.80	15.52	0.82	102.61
	21-3a2	84.65	14.99	0.68	100.98
Twin Bonanza (26022). Gold intergrown with quartz, carbonate and pyrite in early magmatic style veining with similar bismuthinite paragenesis.	22-a1	80.79	19.58	0.52	100.98
	22-a2	80.01	21.38	0.64	102.17
Old Pirate (26023). Gold inclusions in quartz and intergrown with chalcopyrite, arsenopyrite and galena in biotite-rich metamorphosed quartz + carbonate vein.	1a1	88.43	11.51	0.77	101.23
	1a2	94.49	3.15	1.04	98.87
	1b1	77.90	17.75	0.87	97.02

Chemical analyses of gold grains have been obtained from the ore samples of this study (26005; Callie, Groundrush, DBS) and those of previous studies (26002; Hyperion, 26003; Titania, 26023; Old Pirate and 26021; Twin Bonanza). The chemical analyses have been summarised in terms of wt% Au, wt% Ag and wt% Bi (Table 5, Figure 1 and Figure 2). Analyses of gold grains found in association with intrusion hosted mineralisation at Twin Bonanza have been included for comparison.

There is considerable variation in silver content of the gold grains between prospect/deposit areas, with some gold grains clearly better classified as electrum (DBS, Hyperion, Old Pirate and Twin Bonanza). The silver content of the gold grains to some extent defines the prospect/deposit areas and domains within those deposits (i.e. Magpie Schist and Lower Blake Beds within the Callie

deposit). In some examples there is considerable variation in the silver content of gold grains from the same prospect/deposit (Old Pirate, Twin Bonanza) and in the same paragenetic association within the prospect/deposit.

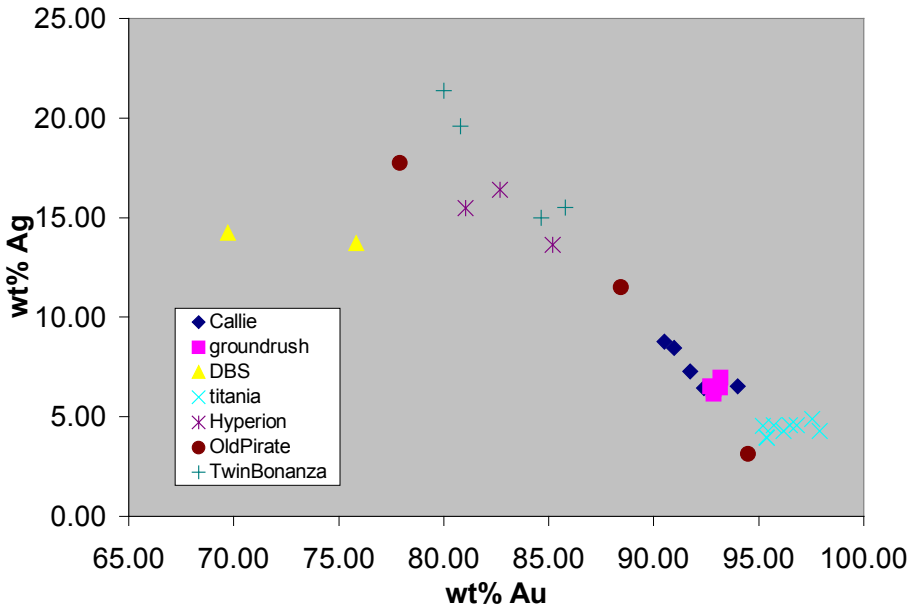

Figure 1. Silver and gold contents of gold (alloy) grains from respective deposits/prospects.

All gold grains contain some amounts of bismuth, between 0.39 wt% and 1.20 wt%, but only in the gold paragenesis at Hyperion is bismuth bearing gold intergrown with bismuth minerals (native bismuth, bismuth tellurium sulphides, and platinum bearing iron-bismuth sulphides). Across the different prospects there is very little variation in bismuth content, and in particular there does not appear to be any higher bismuth content in gold grains intergrown with complex bismuth minerals at Hyperion.

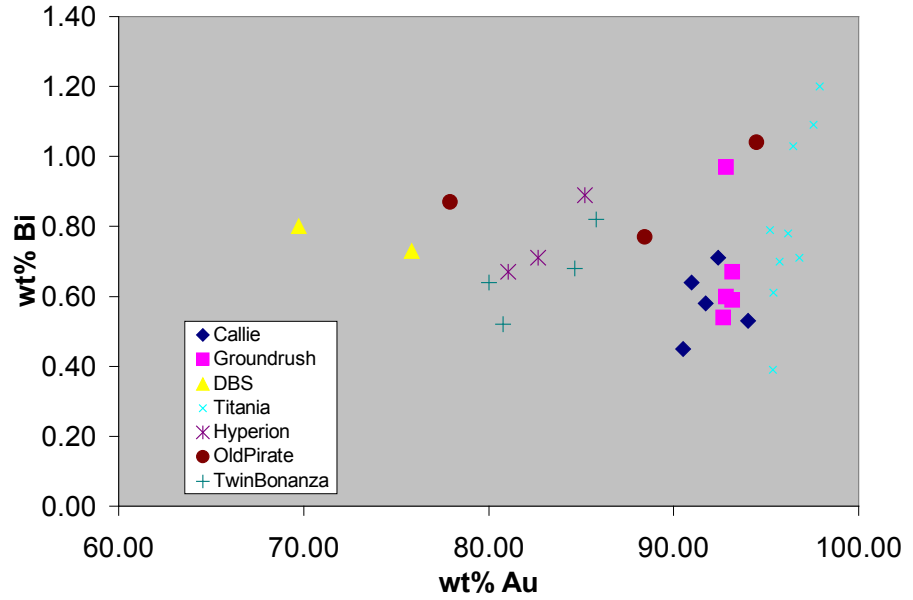

Figure 2. Bismuth and gold contents of gold (alloy) grains from respective deposits/prospects.

BIOTITE CHEMISTRY

TABLE 6. BIOTITE CHEMISTRY (SUMMARISED FROM APPENDIX 3)

Paragenesis	Analysis	K_2O wt%	Cl wt%	F wt%	TOTAL	XMg	IV(F)	IV(F/Cl)
Lower Blake Beds ore zone (26005). Biotite	6.1d	8.24		0.00	93.61	0.345		
intergrown with quartz and K-feldspar	6.1e	8.83	0.02	0.18	95.05	0.358	2.294	4.985
at vein margin with biotite enclosing gold.	6.1f	8.31	0.02	0.37	95.88	0.356	1.984	4.667
Magpie schist, ore zone (26005).	3.4 a	9.39	0.02	0.18	95.60	0.347	2.286	4.955
Biotite intergrown with quartz, muscovite	3.4 b	8.04	0.04	0.34	94.25	0.340	1.961	4.957
and K-feldspar in vein at vein-wallrock	3.4 c	8.01	0.01	0.74	95.12	0.327	1.583	3.984
margin.	3.4 d	7.41	0.03	0.22	91.42	0.346	2.159	5.036
Magpie schist, ore zone (26005). Biotite in	4.1b	8.29	0.01	0.29	96.41	0.324	2.027	4.387
vein quartz enclosing grains of galena.	4.1c	7.20	0.03	0.76	94.11	0.337	1.577	4.478
Groundrush, ore zone, in pit (26005).	9.2a	8.72	0.03	0.27	95.22	0.358	2.169	5.027
Biotite intergrown with chlorite and K-	9.2b	8.87	0.01	0.53	95.68	0.366	1.859	4.267
feldspar in metamorphosed quartz vein	9.2c	9.00	0.03	0.00	95.59	0.359		
cement.	9.2d	8.79	0.05	0.20	94.36	0.377	2.331	5.423
	9.2e	8.87	0.03	0.00	93.53	0.369		
Bunkers pit, ore zone (26005). Biotite	1b.1a	6.05	0.08	0.81	99.94	0.306	1.581	4.813
intergrown with granoblastic quartz	1b.1b	0.38	0.03	0.26	99.42	0.210	2.076	4.653
and F-bearing amphibole (enclosing gold) at	1b.1c	6.88	0.05	0.37	92.83	0.280	1.896	4.883
vein margin.	1b.1d	7.41	0.07	0.43	94.46	0.285	1.805	4.973
Old Pirate, diamond core (26023,	23-1b2	8.09	0.04	0.79	95.28	0.365	1.647	4.679
OPRC076E). Biotite intergrown with quartz	23-1b3	1.84	0.02	0.55	88.07	0.394	1.745	4.586
and carbonate in metamorphosed gold	23-1a4	8.99	0.03	0.82	93.80	0.375	1.652	4.569
bearing vein assemblage.								

The chemistry of biotite contained within mineralised quartz veins is summarised in terms of F wt%, Cl wt%, K wt%, XMg (Mg/Mg+Fe) and fluorine and chlorine intercept values (IV(F) and IV(Cl)). The respective IV(F) and IV(F/Cl) values (Table 6 above, and Figure 3 and 4 below) are derived according to the methods of Munoz (1984). The IV(F) and IV(Cl) values are effective measurements of enrichment of fluorine and chlorine in biotite which allow for the variation in Mg/Fe ratios in biotite. The intercept values are calculated from chemical analysis, and include corrections for the opposing effects of the Mg/Fe ratio on F=OH and Cl=OH exchange in biotite. Fluorine partitions preferentially into Mg-rich biotite whereas chlorine partitions preferentially into Fe-rich biotite (Munoz, 1984). The lower the intercept value the higher the fluorine (or chlorine) content.

All the biotite grains analysed form part of metamorphic replacement assemblages in the respective metamorphosed vein/cement assemblages. Within any given paragenetic site there is significant variation in fluorine contents of the biotite grains. Some of this variation may be as a result of loss of volatile elements on analysis (as evidenced by significantly lower analysis totals in some cases). In general however it is evident from the data, that for any given XMg (Mg/Fe+Mg) value there is some real variation in fluorine content to suggest that there is true variation in fluorine uptake by biotite independent of Fe/Mg ratio and volatile loss during analysis (Figure 3). The data reveal that there is equal fluorine uptake in biotite with different ratios of iron and magnesium in biotite also suggesting that there is real variation in fluorine uptake independent of Fe/Mg ratios. To some extent the range of XMg and IV(F) values define the biotite from the different prospect/deposit areas. The greatest range in values from a single paragenesis is represented in the analysis of biotite grains from gold bearing veins of hosted by the Magpie schist (Figure 3): All analysed biotite grains are from within the same metamorphosed/metasomatised quartz veining.

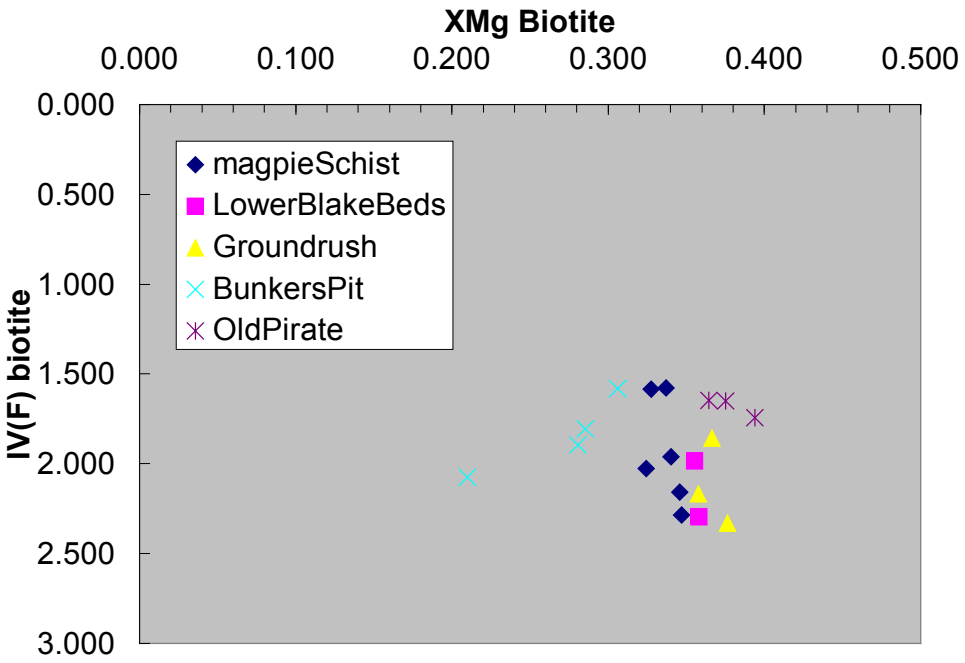

Figure 3. IV(F) and XMg (Mg/Fe+Mg) for individual biotite analyses.

A more or less linear trend in IV(F) versus IV(F/Cl) in biotite analyses is perhaps consistent with opposing avoidance behaviour of fluorine and chlorine with respect to the iron content in biotite (Figure 4). The highest fluorine contents (lowest IV(F) values) correlate with the highest fluorine/chlorine ratios (lowest IV(F/Cl) values). There is no real discrimination of prospect/deposit locations on the basis of IV(F) versus IV(F/Cl) from biotite analyses. Again biotite analyses from the Magpie schist exhibit the greatest spread in values.

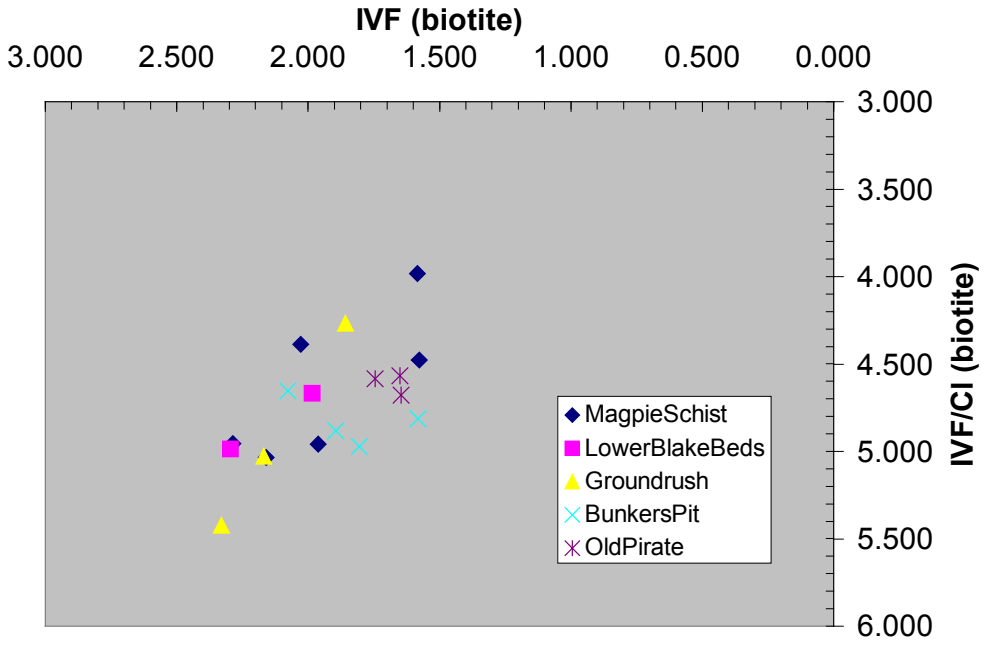

Figure 4. IV(F) and IV(F/Cl) for individual biotite analyses.

A statistical presentation of the IV(F) values from biotite analyses of this study reveals a similar spread of values to those obtained from biotite of similar paragenesis in western Tanami

prospects/projects (Figure 5). A difference in the western Tanami data (Coyote and Pebbles projects) is that some of the biotite analysed included metamorphic biotite in wallrock immediately adjacent to metamorphosed/metasomatised (gold-bearing) quartz veins as well as biotite within the veins. Some intercept values amongst the western Tanami data indicate significantly higher fluorine contents in biotite. Some of these particularly low intercept values (1.3 to 1.5) were obtained from biotite in a single thermally overprinted quartz vein hosted by sandstone (Coyote).

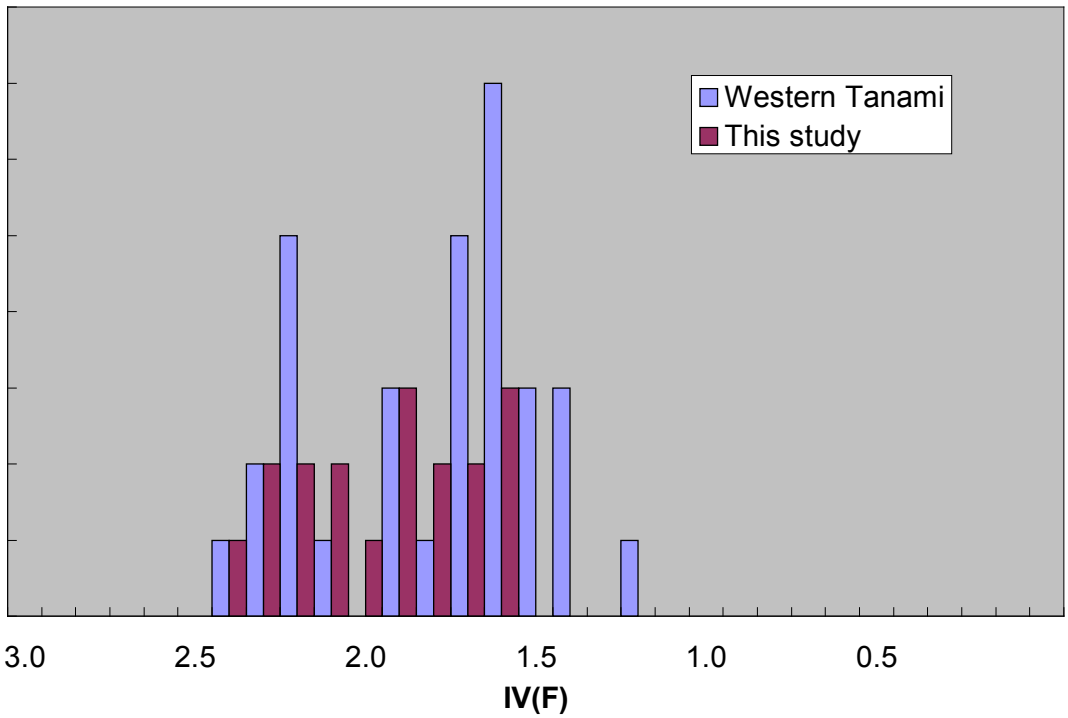

Figure 5. Statistical distribution of biotite intercept values (IV(F)) for biotite grains within metamorphosed/metasomatised vein assemblages of this study, and vein assemblages and marginal wallrock assemblages from western Tanami locations. Relative fluorine enrichment increases to right.

DISCUSSION AND COMMENT

THERMAL OVERPRINTING, RELATED META SOMATISM AND REMOBILISATION OF GOLD

Petrology of gold bearing vein and related wallrock assemblages from the deposit/prospect areas of this study compares favourably with that from other prospect/project areas of previous studies. There is good petrological evidence indicating that varying degrees of metamorphic and related metasomatic overprinting of protore are processes that were common in gold mineralised quartz vein systems across the Tanami region. The preliminary petrological assessments indicate that there is potential for significant remobilisation of ore, potentially upgrading or downgrading ore, as a result of processes of metamorphic and metasomatic overprinting. The distribution of gold and textural relationships with gangue minerals in the metamorphic rock hosted gold deposits of the Tanami, may be explained better by slow fluid transfer rates and slow recrystallisation of thermal metamorphic overprinting of vein assemblages, rather than simple one-stage precipitation from hydrothermal fluid flow. Examples of Tanami gold deposits for which there is little evidence of metamorphic and related metasomatic overprinting include deposits of the Tanami Mine “corridor” and the Pendragon area (although these deposits are tectonically overprinted).

Metamorphic and related metasomatic overprinting and remobilisation of mineralisation are well-recognised processes (Cartwright and Oliver, Marshall et al, 2000). Distances of ore transfer by fluid (Marshall et al, 2000) may be on a scale of centimetres to kilometres and time frames of up to millions of years. More pertinent to the petrology of the Tanami projects is the recognition of the extent of metasomatism associated with thermal metamorphism (Cook and Bowman, 2003; Harris et al, 2002; Sakakibara and Isono, 1996), with the metasomatic fluids derived from dehydration reactions associated with the metamorphism as well as causative intrusions. In some examples of thermal metamorphism, a strong metasomatic fluid flux is determined to be a main contributor to the overall thermal metamorphic effect (Sakakibara and Isono, 1996). In this example a strong hornfels effect characterised by high temperature gradients was strongly manifested by a flux of high temperature fluids. In other cases the extent of hydrothermal fluid generation in thermal metamorphic zones is determined to be instrumental in inducing partial melting, these partial melts ranging from small scale leucosomes to granitoid sheets in migmitite zones (Harris et al, 2002).

Petrological data from the western Tanami provide some clear illustrations of the nature of remobilisation of gold by metasomatic fluids associated with thermal and tectonic overprinting of gold bearing hydrothermal quartz veins (Figures 6, 7, 8, 9 and 10). Mobilisation is represented by discrete secondary fluid inclusion trails (in recrystallised protore quartz) through to discrete "secondary" veinlets (in fact comprising a range of micro-dilational structures) within which hydrothermal textures may be preserved or recrystallised with late thermal re-equilibration. In many examples, discrete secondary fluid inclusion trails link with veinlets, most of which are contained to the metamorphosed framework vein assemblages but also which extend locally into the immediate wallrock.

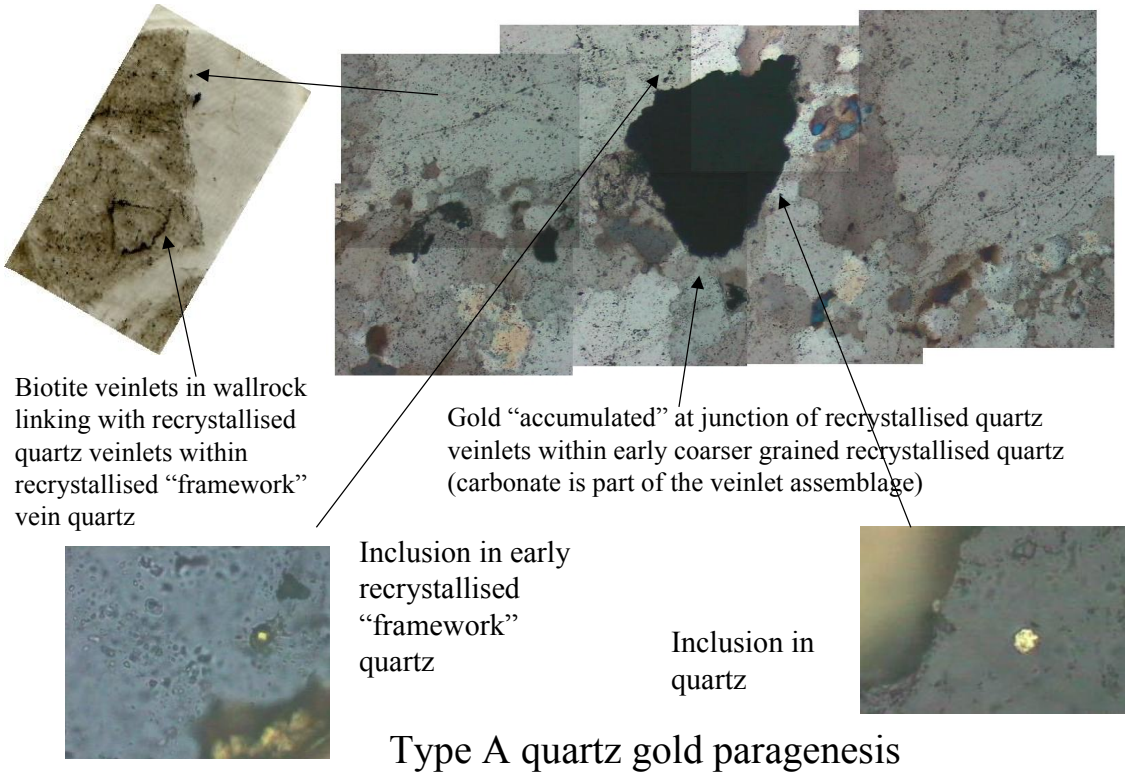

Figure 6. Networks of secondary, compositionally complex fluid inclusions together with gold inclusions as evidence for remobilisation of gold with a metasomatic overprint coincident with and post-dating recrystallisation of protore vein assemblage (western Tanami).

In other studies of metamorphic rocks, the distribution and composition of fluid inclusions hosted by equilibrium metamorphic and metasomatic replacement assemblages have been interpreted to

record the nature of fluids resulting from dehydration reactions of prograde metamorphism (e.g. high pressure moderate temperature domains: Philippot et al 1995). In these examples, it was determined that fluids derived from dehydration reactions were involved in localised as well as distal metamorphism/metasomatism, a concept readily applicable to the metamorphic regime in the Tanami.

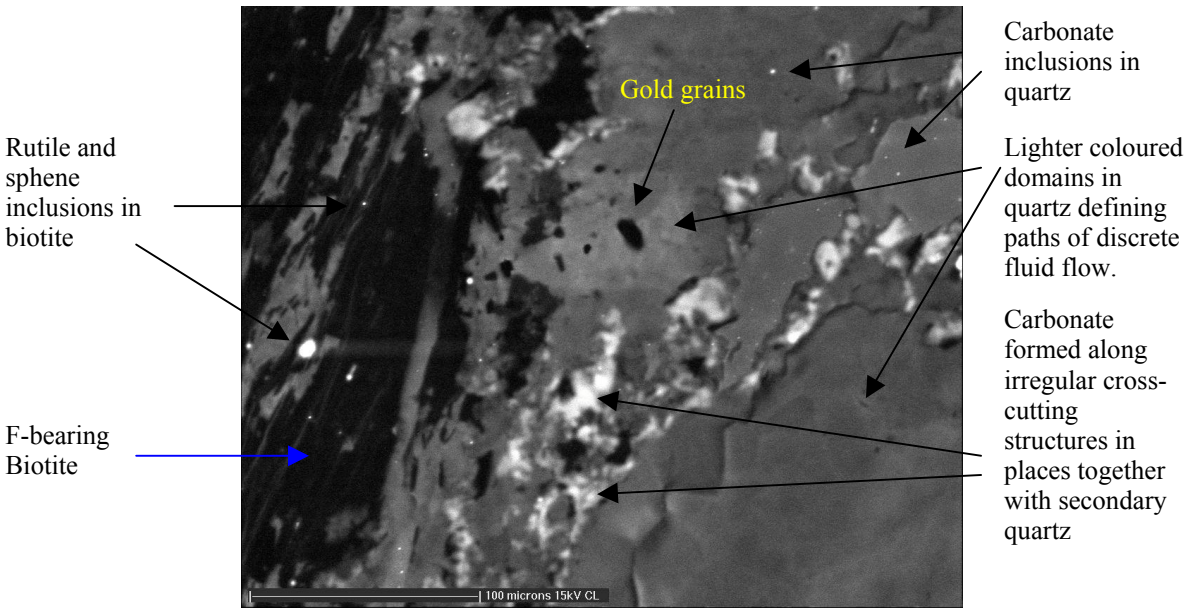

Figure 7. Discrete fluid pathways in recrystallised quartz, as evidenced by cathode illuminescence, along which gold and related elements were remobilised. Different scales of discrete fluid flow are evident. Old Pirate.

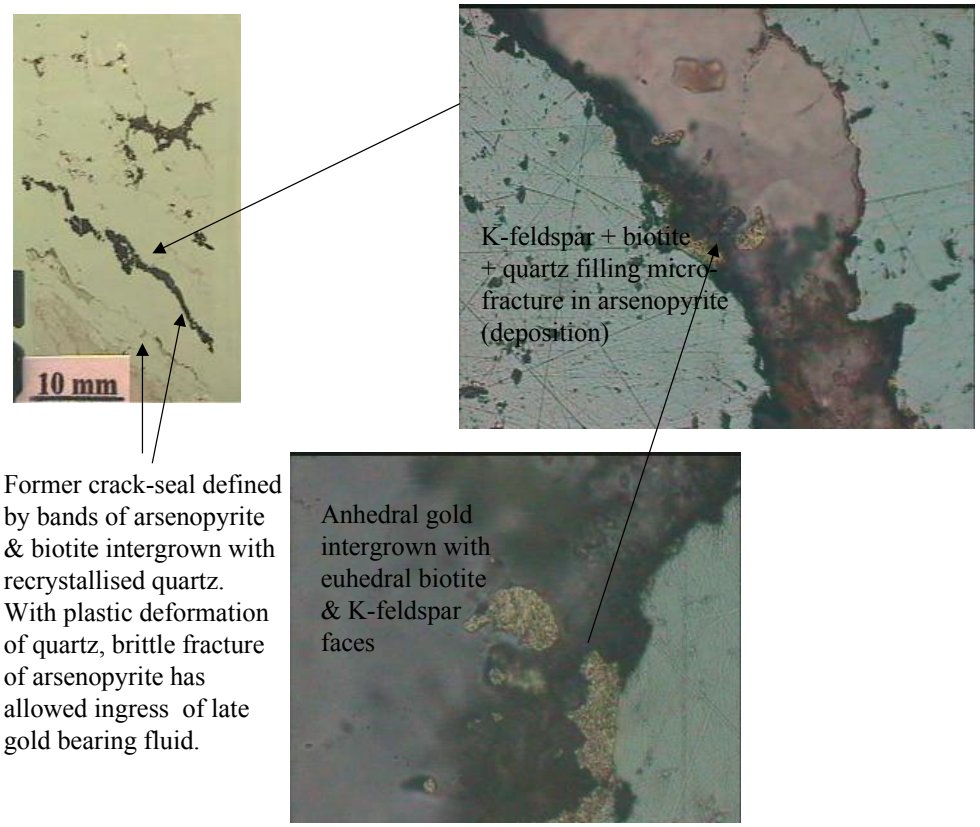

Figure 8. Gold intergrown with quartz, K-feldspar and biotite in more obvious secondary microfractures. Biotite together with gold, K-feldspar and quartz was precipitated from locally derived saline fluids. Western Tanami.

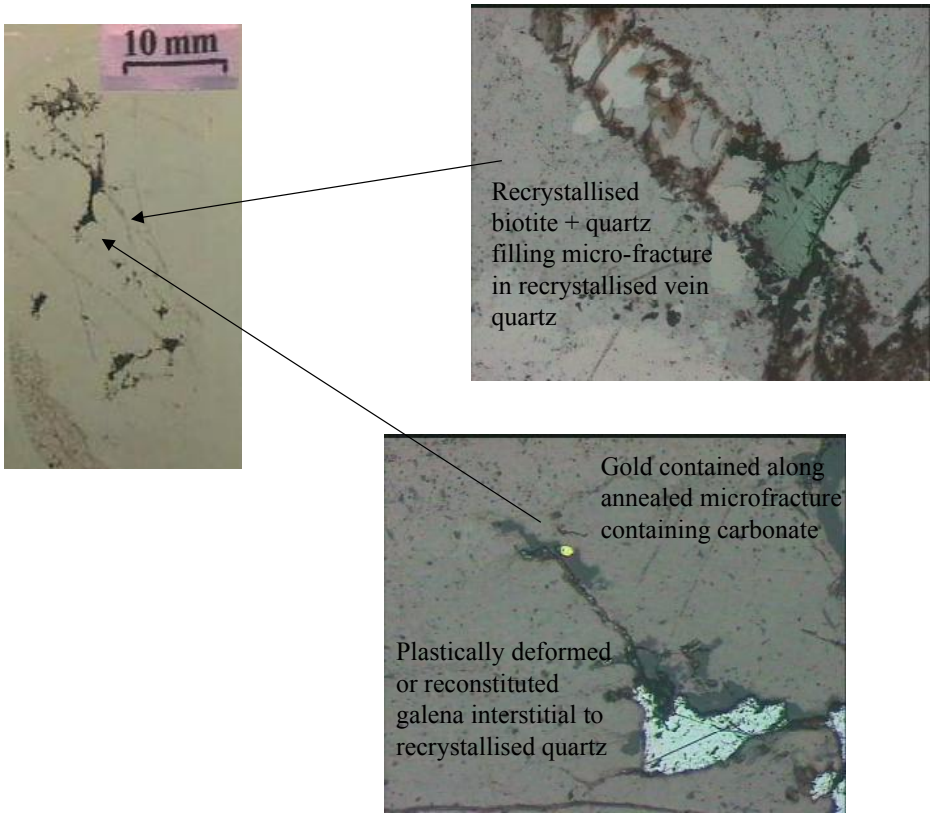

Figure 9. A further example of secondary fluid inclusion trails linking with quartz + biotite + K-feldspar + sulphides veinlets, some including mobilised gold. In this example the secondary vein assemblages are recrystallised within thermal regime overprinting the protore quartz vein.

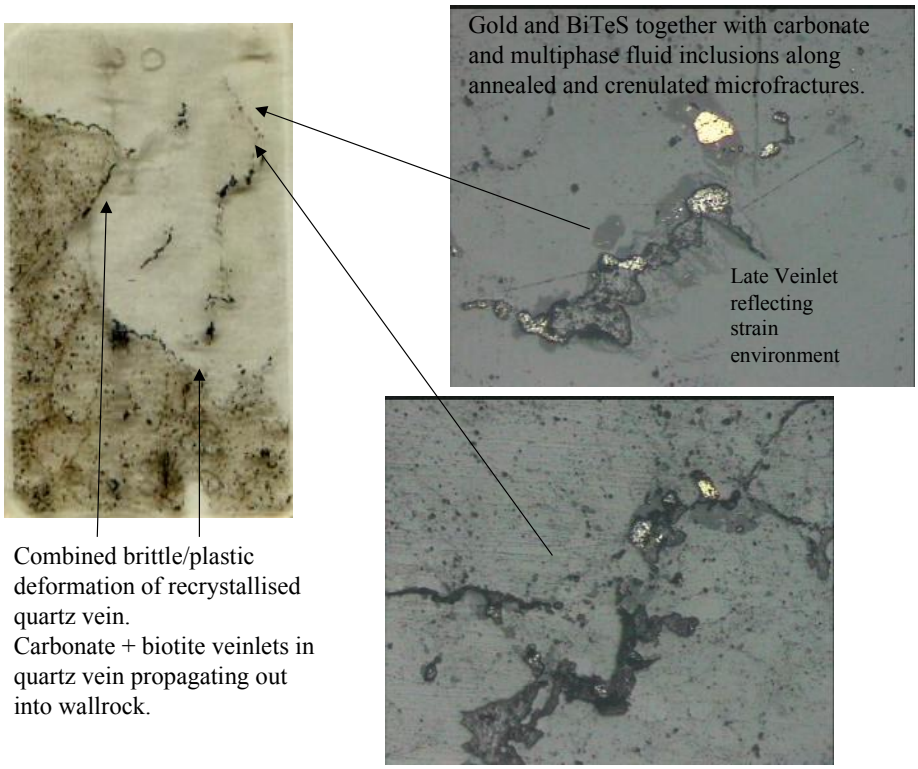

Figure 10. Stylolitic quartz + carbonate + mica + sulphides veinlets traversing recrystallised vein quartz entraining mobilised bismuth and gold, the bismuth possibly mobilised as a melt/liquid.

Partial melting of sulphide assemblages has also been suggested as a mechanism for mobilising and upgrading (or downgrading) ore deposits (e.g. Tomkins et al, 2004, Tomkins and Mavrogenes, 2002), with some sulphosalt partial melting persisting to temperatures below 300 °C. Small-scale mobilisation, but potentially greater mobilisation in conjunction with partial melting of silicate gangue mineralogy may be a factor to consider in the Tanami deposits/prospects. The distribution of some bismuth filled inclusions is to suggest that bismuth behaved as a liquid, in places entraining native gold with it.

DISTRIBUTION OF BISMUTH (IN GOLD AND OTHER MINERALS)

The variation in silver content of gold grains (Table 5 and Figure 1) between the different prospects/deposits is probably a reflection the differences in chemistry of the hydrothermal fluids from which the primary mineralised quartz veins were formed. The local variation in silver content of gold within prospect/deposit locations, with Old Pirate as a good example (Table 5), probably reflects the effects of local metasomatic overprinting.

A positive correlation between bismuth and gold is considered important amongst criteria in the recognition of gold deposits related to reduced granitic intrusions (Thompson and Newberry, 2000), or (as they are termed now) the Intrusion-Related class of gold deposit (Baker and Lang, 2001; Mustard, 2001; Rombach and Newberry, 2001). Amongst other criteria, the presence of bismuth minerals and bismuth geochemistry support the assertion that granitoid hosted mineralisation at Twin Bonanza warrants classification as an Intrusion-Related class of gold deposit. Most readily recognised Intrusion-Related gold deposits are hosted by granitoids. More equivocal amongst reported Intrusion-Related gold deposits are those not directly hosted by granitoids, but those occurring adjacent to what are described or interpreted as being causative intrusions. Where reported Intrusion-Related gold deposits are not hosted by granitoids, more emphasis is placed on ore mineral associations and elemental associations, such as bismuth-gold in asserting Intrusion-Related gold classification.

The thermally metamorphosed and metasomatised gold mineralised quartz vein systems hosted by a range of metamorphic rocks as discussed in this report, are related to granitoid intrusions by way of the thermal overprinting (and associated effects). In question is the source and nature of hydrothermal fluids from which the primary (protore) quartz and related-vein mineralogy precipitated. These fluids may have been metamorphic, magmatic, meteoric or a combination of all three. If a significant component of these fluids was magmatic, either sourced from those intrusions responsible for thermal overprinting or older intrusions, then Intrusion-Related gold deposit classifications might be appropriate. With this in mind it might be significant that amongst the deposit types discussed in this study, at least three have strong mineralogically defined gold-bismuth (+ tellurium-silver) associations. At Hyperion, Coyote and Pebbles (western Tanami), native gold and electrum are locally intergrown with complex bismuth-telluride-sulphide minerals. Similar bismuth-telluride-sulphide minerals have so far not been identified in veining at any of the other deposits/prospects of this type (as discussed in this report). This may in fact simply be the result of an irregular distribution of the bismuth-telluride-sulphide minerals within (and possibly a consequence of) the thermally overprinted and metasomatised nature of the vein assemblages. It might be significant to note that in the examples of Tanami prospects where bismuth-tellurium-sulphide minerals are present, gold always occurs with the bismuth-tellurium-sulphide mineralogy, but bismuth-tellurium-sulphide minerals do not always occur with gold.

A feature of prospects/deposits that do have bismuth-tellurium-sulphide minerals present, is the bismuth content of associated gold/electrum. As an example, gold intergrown with complex

bismuth-tellurium-sulphide minerals at Hyperion contains between 0.67 and 0.89 wt% bismuth (Table 5). Although not of the same style of deposit, gold with a relatively close spatial association with bismuth mineralogy at Twin Bonanza contains between 0.52 and 0.82 wt% bismuth. Some parts of the Titania deposit have strong bismuth (whole-rock) geochemistry but as yet no bismuth minerals have been identified. Gold grains from the Titania deposit do however contain between 0.39 and 1.20 wt% bismuth. In other deposits of this study for which bismuth-tellurium-sulphide minerals have not been identified the bismuth content of gold/electrum grains is comparable to those from deposits/prospects that do contain bismuth-tellurium-sulphide mineralogy. This observation might lead to the suggestion that in the absence of identification of bismuth mineralogy or whole-rock geochemistry, the bismuth content of gold might be an indicator of the extent of a gold-bismuth association within the prospect/deposit.

In summary, further investigation is required before the usefulness of bismuth content of gold/electrum can be rationally assessed as a paragenetic indicator and ultimately whether it can be used as a guide to magmatic hydrothermal fluid associations. The bismuth content of gold from a range of different deposit types, including those for which it is unequivocal that there is not a relationship with intrusions, would be useful.

ORIGIN, DISTRIBUTION AND SIGNIFICANCE OF FLUORINE ENRICHMENT IN BIOTITE

Studies of fluorine and chlorine exchange with hydroxide in biotite (and other mica minerals) has applications to hydrothermal ore deposits (Munoz, 1984; Finch, 1985; Philippot et al, 1995; Coulson et al, 1999; Osani et al, 1996). The studies of fluorine and chlorine enrichment in hydrothermal (and late-stage igneous) biotite are used to calculate or interpret activities of the halogens within hydrothermal fluids in equilibrium with biotite. As indirect measurements or guides to activities of fluorine and chlorine in hydrothermal fluids, the halogen content of biotite can have importance from the point of view of their role in ore-forming processes (e.g. chlorine complexing). More generally, as a guide to halogen activity in hydrothermal fluids, the fluorine and chlorine content of biotite has been used to make interpretations about hydrothermal environment including source of fluids.

In relation to studies of the gold-mineralised Emerald Lake pluton, Yukon Territory, Canada, fluorine contents of late stage magmatic (monzonite and syenite) biotite and related pegmatite were determined to be in the range 1.5 to greater than 2.2 wt% (Coulson et al, 2001). These values are somewhat higher than fluorine contents determined for biotite associated with quartz veining presented in this study (Table 6). The fluorine content of biotite was studied in relation to the metasomatic overprinting of pyroxene-bearing igneous rocks by magmatic fluids sourced from younger syenite rocks at Igdlerfigsalik, south Greenland (Finch, 1995). In the Igdlerfigsalik example, the fluorine content of metasomatic biotite (after pyroxene) falls within a similar range of the values obtained for the quartz vein-related biotite (for similar Fe/Fe+Mg ratios) of this study (Table 6). Perhaps more useful in comparing fluorine enrichment in biotite between hydrothermal (and igneous) environments is in a statistical analysis of fluorine intercept values (Munoz, 1984). Comparisons involving fluorine intercept values (IV(F)) will take into account the different Mg/Fe + Mg ratios in biotite that strongly affects fluorine exchange in biotite.

A comparison of fluorine intercept values for biotite from metamorphosed/metasomatised quartz veins from the Tanami with values from other hydrothermal and igneous settings (compiled by Munoz, 1984) is presented in Figure 11. The data of Munoz (1984) reveals an overlap between igneous biotite and hydrothermal biotite, and highest fluorine enrichment associated with a porphyry molybdenum deposit. The presentation of data also indicates that fluorine enrichment in

the biotite from metasomatised/metamorphosed, gold bearing veins from the Tanami is similar to that for igneous rocks and other mineralised magmatic related hydrothermal systems (Figure 11).

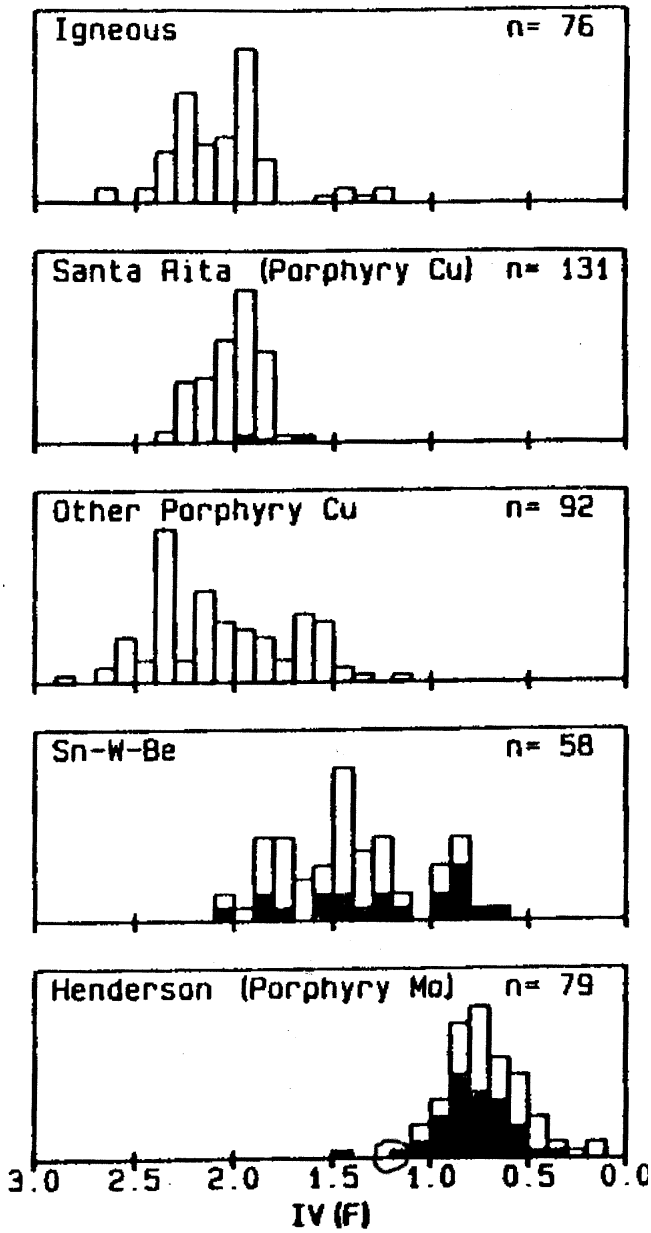

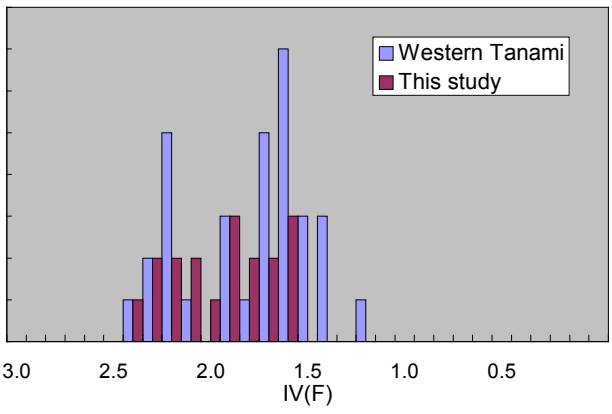

Figure 11. Statistical representation of IV(F) for biotite analyses of this study compared with similar data for other mineral deposit types/associations compiled by Munoz (1984). As with figure 5, relative enrichment in fluorine increases to the right. The shaded areas in the Munoz data are for sericite and muscovite.

The data as presented in Figure 11 tends to suggest that the relatively fluorine enriched biotite of Tanami metamorphosed/metasomatised quartz veins, represent modifications of hydrothermal systems in the history of which there was some magmatic fluid influence. Considering that the biotite analysed represent metamorphic and metasomatic overprinting of protore vein (and associated wallrock replacement) assemblages, the timing of the magmatic fluid influence and fluorine enrichment is therefore perhaps an issue. In one scenario, the fluorine enrichment in the metasomatic/metamorphic biotite may represent an inherited enrichment in mica minerals, possibly sericite and chlorite, formed during hydrothermal flow from which the primary vein and hydrothermal alteration assemblages were formed. Alternatively the relative fluorine enrichment in the biotite may represent the introduction of magmatic fluids, possibly as a volatile component-only (HCl, HF, H_2S, SO_2 etc), during the thermal metamorphic and metasomatic overprinting stage. In the latter scenario the implication is that magmatic volatile components derived from an intrusion causative to thermal metamorphism, mixed with metasomatic, aqueous and CO_2-rich fluids derived from local prograde dehydration reactions. In either scenario the local variations in fluorine enrichment in biotite could be explained by metasomatic and metamorphic overprinting of primarily fluorine enriched hydrothermal sericite and chlorite, or late introduction of fluorine during metasomatic and thermal metamorphic overprinting. The relative enrichment of fluorine in biotite is consistent with the presence of apatite in the recrystallised vein assemblages.

Little is documented in the way of the fluorine contents of metamorphic biotite. Average fluorine contents of metamorphic biotite are reported to be around 0.2 wt%, for biotite with average Mg/Fe + Mg ratios (Quidotti, 1984). Sources of non-magmatic fluorine entrained within metasomatic fluid might have included detrital apatite and muscovite. While there are significant amounts of detrital muscovite and trace amounts of detrital apatite in Tanami metasedimentary rocks (host to mineralisation), both these phases were stable within the peak metamorphic/metasomatic regimes, and are unlikely sources of fluorine in hydrothermal fluids. Levels of fluorine enrichment, similar to those of the Tanami examples, are reported in biotite in high pressure moderate to high temperature metamorphic rocks from the Dora-Maira massif, Western Alps (Philippot et al, 1995). Fluorine enrichment in biotite in rocks from the Dora-Maira massif have been ascribed to the formation of the host mica minerals in the presence of aqueous fluids derived from dehydration reactions which took place in pelitic rocks interbedded with evaporite deposits. Evaporite deposits are not known or preserved amongst the Tanami stratigraphy and nor is detrital fluorite identified, and therefore a sedimentary source of fluorine is unlikely.

Consistent with relative enrichment of fluorine in biotite of metamorphosed/metasomatised quartz veining, is the presence of relatively abundant rutile within the same vein assemblages. It has been revealed that dehydration-reactions involving fluorine bearing micas favours the hydrothermal transport of Ti in the resulting metasomatic/hydrothermal fluids (Osani et al, 1996). I could be that elevated levels of fluorine in the metasomatic overprinting fluid facilitated mobilisation of Ti from the immediately adjacent wallrock to the metamorphosed/metasomatised vein assemblages.

IMPLICATIONS FOR GOLD EXPLORATION

i). Alteration

Where metamorphic and metasomatic overprinting is a factor, alteration primarily related to hydrothermal quartz veining will not be obvious, in fact obscured. A feature of the metamorphosed and metasomatised, gold mineralised quartz vein systems of the Tanami is an absence of well-defined alteration halos. This absence of alteration halos is a function of the thermal/metasomatic overprinting which in theory has replaced probable early sericite + chlorite + carbonate alteration

with biotite + muscovite + chlorite + carbonate (or higher grade calc-silicate mineralogy) relatively indistinguishable from peak metamorphic replacement of surrounding low grade regionally metamorphic rock. The presence of retrograde alteration, comprising more obvious sericite and chlorite formed along late brittle fracturing and more subtle shearing often coincident with the high-grade vein assemblages may mislead.

ii). The "Nugget" Effect

Gold has affinity for itself and within the scope of the model of metasomatic mobilisation of gold discussed in this and previous reports, there will be local concentration of gold in quartz veins where primarily it might have been evenly distributed throughout. Such remobilisation and concentration of gold can explain high-grade intersections that cannot be repeated in "twin" drill holes, or why quartz veining can be correlated between intersections but gold grade cannot. Establishing early on in a prospect exploration programme that there is a primary "nugget" effect in gold distribution could be important in determining how the prospect is explored and evaluated. Differentiating between a primary and supergene nugget effect could be important in the interpretation of early drilling results: a supergene nugget affect will be confined to a near surface environment, whereas a primary nugget effect is likely to persist with depth.

iii). Significance of Host Rock Types

The nature, abundance and combination of rock types within a prospect or potential prospect area could determine whether an upgrade of ore could have occurred as a result of metasomatic overprinting. The presence of voluminous pelitic beds (represented primarily by hydrous regional metamorphic chlorite) could have been important for generation of secondary fluids with which to mobilise and concentrate gold. While still confined to (metamorphosed/metasomatised) quartz veins (and marginal wallrock), through processes metasomatic remobilisation, gold (and related minerals) could have become concentrated within certain strata. The preferred strata, may not necessarily be that from which the majority of the mobilising metasomatic fluids were derived, but a stratigraphic unit favouring re-precipitation of gold. Processes of metasomatic remobilisation are likely to have been more effective in concentrating gold in sheeted protore veining hosted by alternating sandstone and mudstone than they would in the same volume of veining, hosted by monotonous siliceous sandstone. Metasomatic remobilisation in association with metamorphic overprinting could be considered a better explanation of strata-bound mineralisation, especially where mineralised quartz veins are at high angles to the mineralised and non-mineralised host rock sequence. There will have been relatively no time limit to the processes of metasomatic remobilisation and ore upgrade, compared to the time of protore emplacement limited by the life of the primary hydrothermal system.

More locally, carbonaceous beds within any host rock sequence will have been an important source of sulphur required for bisulphide complexing and remobilisation of gold. The presence of carbonaceous beds will have facilitated the buffering of circulating fluids to low fO_2 conditions, such that in rocks containing pyrite or other sulphides, H_2S was the predominant form of sulphur. Carbonaceous material was the likely source of H_2S, either by leaching or break down of organic sulphur compounds. Hot fluids moving through the carbonaceous and pyritic rocks should be H_2S-rich and capable of scavenging gold and transporting it to sites of ore deposition. Also important might have been some meta-sediments host to residual NaCl, which could have been accessed by metasomatic fluids and also utilised in the remobilisation of gold as chloride complexes. Excess sulphur could have been derived from other processes such as the conversion of pyrite to pyrrhotite with thermal overprinting. Local decarbonation of metasediments, in conjunction with

remobilisation of gold, could have been achieved by metasomatic fluids generated during thermal overprinting according to the reaction:

$$2C + 2H_2O = CH_4 + CO_2$$

The complexity of secondary fluid inclusions genetically related to metasomatic overprinting, including CH_4 and CO_2 types (e.g. at Callie and Coyote), is evidence of such reactions.

iv). Metamorphic Grade

The extent to which metasomatic fluids could have been generated, as a result of dehydrated reactions with metamorphic overprinting will have varied with metamorphic grade. If the grade of metamorphic overprinting was too low (or non-existent) there will have been little potential for metasomatic fluid generation and ore mobilisation and upgrade. At the other end of the scale, higher grade metamorphism with excessive fluid generation could lead to partial melting of ore and enclosing rock resulting in another mechanism of ore mobilisation and concentration. In the case of voluminous partial melting, aqueous fluids and gold may be have become entrained within the partial melt and only exsolved upon crystallisation of the partial melt. At higher grades of thermal metamorphic overprinting, a more ductile style of deformation will have prevailed such that penetrative permeable pathways necessary for extensive fluid mobilisation of ore may not have been possible. In summary, there may have been an optimum grade of thermal metamorphic overprinting for ore mobilisation and effective upgrade.

v). Metallurgy

Where the gold protore comprised refractory gold in pyrite (either as metallic grains or tied up in the pyrite lattice), thermal metamorphic and related metasomatic overprinting will have resulted in a release of the gold. As an example, thermal overprinting of pyrite host to refractory gold might produce in an assemblage comprising metallic gold + pyrrhotite (with sulphur as a by-product). In terms of the thermal overprint resulting in more recoverable gold, this in effect is an ore upgrade. As discussed earlier in this report, the gold deposits of the Tanami corridor are examples of Tanami gold mineralisation that has not been subjected to significant thermal (and/or metasomatic) overprint. A feature of these gold deposits is the highly refractory nature of the gold ores (at least below the level of oxidation), and in the context of other Tanami deposits, this is probably a consequence of these deposits not having being subjected to any significant thermal/metasomatic overprinting.

vi). Igneous association

There are some valid economic considerations in determining whether or not (by way of bismuth chemistry, biotite chemistry and/or any other constraints) the style of metamorphosed and metasomatised style of gold deposits discussed in this report might be intrusion related. In the first instance, if only some of these deposits are genetically related to intrusions the prospectivity of these deposit types might be quite different to those, which are genetically related to broader scales of metamorphic hydrothermal fluid generation.

There may in fact be both a narrow and broader context of intrusion related mineralisation to consider. In the narrow context, these metamorphosed/metasomatised gold deposit types, similar to those hosted by granitoids (i.e. Twin Bonanza), might have primarily been formed from hydrothermal fluids mainly exsolved from granitoid intrusions. In this case, determination of

which granitoid types are associated with prospective gold deposits will be important. In the broader context, metamorphic fluids generated deep within the crust and giving rise to economic gold deposits, may also have been instrumental in generating granitic melts which when emplaced ultimately give rise to the thermal metamorphic and related metasomatic overprinting. These granitic (or other composition) intrusions are in effect samples of the lower crust from which the precursor ore fluids were generated and as such their petrogenetic signature could be indicative of the prospectivity of surrounding rocks.

Of course there should be consideration of the structural controls granitoid intrusions might have played in localising the primary gold mineralised quartz vein systems. If the granitoid intrusions are indeed causative to the thermal and metasomatic overprinting, then there are timing issues if the granitoids were to have had any structural influence on the localisation of those primary quartz vein systems.

PETROLOGY 2005

Ongoing Prospect Evaluations

i). Lithoteque Database.

There could be a need to create a lithoteque database that would specifically illustrate and demonstrate the petrological features pertinent to the model of metasomatic overprinting of mineralised quartz veining in association with variable thermal metamorphic overprinting. Appropriate written descriptions and interpretations should form part of the lithoteque. Vein textures, some in relation to remobilised/localised gold, and wallrock including metasomatic and thermal overprint textures should be included in the lithoteque.

A similar lithoteque should be created for what is known of unequivocal intrusion related/hosted mineralisation in the Tanami, with Twin Bonanza as the obvious example.

ii). Prospect characterisation.

Petrological evaluation of prospects should be undertaken at the earliest possible time to assess key features of the prospect, including aspects of rock types, metamorphism, metasomatism, gold association etc, in terms of available models. The models relevant to the Tanami being, intrusion hosted/related deposits such as Twin Bonanza, and the variably metamorphosed and metasomatised vein/lode deposits (focus of this report) which may or may not necessarily be intrusion related.

These petrological evaluations should comprise carefully selected samples, with more work on fewer samples as opposed to less work on many samples, as a cost-effective measure. A review of sample selection criteria for field geologists and what can be gained from petrology (beyond rock and alteration types) should perhaps be undertaken. An understanding of models and petrological techniques is required.

Deposit Model Development, Processes Recognition and Development/Refinement of Petrological Tools

i). Bismuth and gold geochemistry.

As part of the pursuit of criteria useful in the discrimination of deposits that might be genetically related to intrusions, a review of the literature related to natural bismuth contents of gold would be useful. More specifically the objective should be to determine what is the distribution of bismuth in gold and significance in terms of deposit classification, and in the absence of bismuth minerals does the bismuth content of gold reveal anything of the petrogenesis of gold deposits.

ii). Biotite chemistry.

As a tool in the discrimination of fluid types, fluid histories and fluid sources, further work could be undertaken on biotite chemistry and evaluation as to its suitability as a cost-effective petrological tool. As part of this work the chemistry of groundmass and early secondary biotite in rocks of the Twin Bonanza deposit should determined for correlation and comparison with biotite associated with the thermally metamorphosed and metasomatised lode gold deposits (this study).

iii). Xenotime/monazite dating of vein assemblages.

Thought could be given to the potential of U/Pb dating of xenotime/monazite by the method of cost-effective electron microprobe analysis. Xenotime (and possibly monazite) is regularly observed in metasomatised and thermally overprinted gold mineralised quartz veins. The paragenesis of these complex Y, U and Pb bearing minerals is such that they provide a basis for dating the metasomatic overprint to the gold bearing quartz veins, and therefore date of remobilisation and any ore upgrade. A comparison of U/Pb dates obtained from xenotime grains in metamorphosed/metasomatised quartz veins with U/Pb dates obtained from zircon in granitoid inclusions would be useful in refining the model of metamorphosed/metasomatised protore.

iv). Metasomatic fluid flow modeling (and remobilisation of ore minerals).

Further research could be carried out to determine the potential scale of ore mobilisation associated with metasomatic and thermal overprinting, and the extent to which secondary fluids and thermal elevation could be involved in generating partial melting of sulphide assemblages. The model requires more proof. Some of this research could involve geochemical modeling of the metasomatic fluid flow in conjunction with a review of (extensive) existing fluid inclusion data. The multiphase and compositionally complex fluid inclusion populations reported would appear to be consistent with overprinting metasomatic fluids generated locally within host rocks. As part of this work, modeling of the fluid types that might be generated within the different rock types could be undertaken. Additional thermometry based on phase equilibria could be used to constrain thermal overprinting and associated fluid generation, and potential for partial melting of sulphide assemblages.

As part of any metasomatic fluid flow modeling, there should be an integration of petrology and existing geochemical studies: Can the existing geochemical data/studies be explained in terms of thermal metamorphic and metasomatic overprinting, more particularly metasomatic overprinting? Niche geochemical studies of sample suites from Callie have some associated petrographic/mineragraphic work, but this petrography/mineragraphy requires integration with the broader petrological database.

v). Petrological interpretation of geophysical data

More could be achieved in the application of micro-structural and petrological data to regional structural interpretations. The development of thermal metamorphic isograd modeling has probably been taken as far as it can, given the distribution of useful petrological data. A very useful exercise would be in the separation of pre-thermal and post thermal metamorphic structures, as defined by regional geophysical data. According to the thermal overprint model, those structures that will have primarily facilitated and localised mineralisation will pre-date intrusion emplacement, and will have suffered some amount of ductile deformation and in fact will be relatively subtle. Those that post date mineralisation and thermal overprinting associated with intrusion emplacement will most likely be more penetrative (reflecting a more brittle structural regime) and cross-cut and displace intrusions and associated thermal domains.

Further interpretation of geophysical data could also be used in identifying domains of favoured secondary fluid generation and upgrading/concentration of gold ore: i.e. meta-rock types.

vi). Techniques in hydrocarbon petrology.

There is scope for the application of hydrocarbon techniques in understanding hydrothermal environments and temperatures of secondary metasomatism. A combination of vitrinite reflectance and fluorescence techniques is an example.

REFERENCES

Osanai, Y., Hensen, B.J. and Owada, M., High-temperature dehydration melting of fluorine-bearing biotite in pelitic compositions: Experimental investigation and application to granulites. 30th International Geological Congress, Beijing (China), Aug 1996.

Philippot, P., Chevallier, P., Chopin, C., Dubessy, J., 1995. Fluid composition and evolution in coesite-bearing rocks (Dora-Maira massif, Western Alps): implications for element recycling during subduction. Contrib mineral Petrol 121:29-44.

Finch, A., 1995. Metasomatic overprinting by juvenile igneous fluids, Igdlerfigsalik, south Greenland. Contrib Mineral Petrol, 122:11-24

Sakakibara, M., and Isono, Y. 1996. Middle Miocene thermal metamorphism due to the infiltration of high-temperature fluid in the Sanbagawa metamorphic belt, southwest Japan. Contrib Mineral Petrol 125:341-358.

Harris, N., McMillan, A., Holness, M., Uken, R., Watkeys, M., Rogers, N., Fallick, A., 2002. Melt Generation and Fluid Flow in the Thermal Aureole of the Bushveld Complex. *J. Petrology* 44: 1031-1054.

Cook, S.J., Bowman, J.R., 2003. Mineralogical Evidence for Fluid–Rock Interaction Accompanying Prograde Contact Metamorphism of Siliceous Dolomites: Alta Stock Aureole, Utah, USA *J. Petrology* 41: 739-757.

Marshall, B., Vokes, F.M., Larocque, A.C.L., 2000. Regional Metamorphic remobilisation: Upgrading and formation of ore deposits. In Reviews in Economic geology, V II.

Cartwright, I., Oliver, N.H.S., 2000. Metamorphic fluids and their relationship to the formation of metamorphosed and metamorphogenic ore deposits. In Reviews in Economic geology, V II.

Tomkins, A.G., Pattison, D.R.M., Zaleski, E., 2004. The Hemlo Gold Deposit, Ontario: An example of melting and mobilisation of a previous metal-sulphosalt assemblage during amphibolite facies metamorphism and deformation. Economic Geology, vol99:1063-1084.

Tomkins, A.G., Mavrogenes, J.A., 2002. Mobilisation of gold as a polymetallic melt during pelite anatexis at the Challenger Deposit, South Australia: A metamorphosed Archean gold deposit. Economic Geology vol 97: 1249-1271.

Munoz, J.L., 1984. F-OH and Cl-OH exchange in micas with applications to hydrothermal ore deposits. Reviews in Mineralogy. Vol 13: 469-493.

Quidotti, C., 1984. Micas in metamorphic rocks. Reviews in mineralogy. Vol 13: 357-456.

Thompson, J.F.H., Newberry, R.J., 2000. Gold deposits related to reduced granitic intrusions. Reviews in Economic Geology. Vol 13;377-400.

Lang, J.R., Baker, T., 2001. Intrusion-related gold systems: the present level of understanding. Mineralium Deposita,. Vol 36:377-489.

Mustard, R., 2001. Granite-hosted gold mineralisation at Timbarra, northern New South Wales, Australia. Mineralium Deposita. Vol 36:542-562.

Coulson, I.M., Dipple, G.M., Raudsepp, M., 1999. Evolution of HF and HCL activity in magmatic volatiles of the gold-mineralised Emerald Lake pluton, Yukon Territory, Canada. Mineralium Deposita. Vol. 36:594-606.

Rombach, C.S., Newberry, R.J., 2001. Shotgun deposit: granite porphyry-hosted gold-arsenic mineralisation in southwestern Alaska, USA. Mineralium Deposita. Vol 36:607-621.

APPENDIX ONE:

PETROGRAPHIC/MINERAGRAPHIC DESCRIPTIONS

SAMPLE NUMBER: 26005.1a
LOCATION: Bunkers ore zone
ROCK NAME: Thermally metamorphosed quartz vein and meta-sedimentary rock.
FIELD DESCRIPTION: A quartz veined metasediment

OFFCUT DESCRIPTION:

The rock is of mottled dark grey and brown-yellow, quartz veined, metasediment. A cement dominated by vitreous, grey to grey-brown vein quartz encloses slivers of dark grey, crystalline, well-cleaved metasediment. The wallrock and vein assemblage, are moderately to strongly weathered. As part of the weathering, a pervasive yellow mineral has formed after the vein assemblage.

THIN SECTION DESCRIPTION

LITHOLOGY: PRIMARY MINERALOGY, TEXTURES

The distribution metamorphic replacement minerals preserves a primary sedimentary lamination or bedding structure. A former laminated siltstone texture is indicated by the grain-size variation within the metamorphic replacement assemblage.

ALTERATION

REPLACEMENT

Replacement is complete. The metamorphic replacement assemblage is dominated by fine grained, tabular to prismatic green-brown-blue amphibole. Minor to moderate amounts of ghosted biotite and orthopyroxene are interlocking with the amphibole and anhedral quartz is interstitial to the preserved and ghosted silicate minerals. In some places, brown biotite is relatively well preserved. Minor to trace amounts of muscovite and clinopyroxene are intergrown with the silicate minerals. The clinopyroxene is most intimately associated with the ghosted/pseudomorphed orthopyroxene. The ghosted/pseudomorphed orthopyroxene is host to ghosted, tabular, euhedral opaques and/or spinel minerals. Trace amounts of ultra fine-grained pyrite and pyrrhotite occur as inclusions within or interstitial to the metamorphic replacement minerals.

The orthopyroxene is replaced by fibrous to platy secondary minerals, probably clays. The opaque or spinel minerals are replaced by very fine to ultra fine-grained hematite locally colloform banded.

DEPOSITION

The metamorphic wallrock material is fractured and filled/cemented with anhedral, tabular, fine to medium grained quartz. The quartz has widespread undulatory extinction. Grains of green-brown-blue amphibole, clinopyroxene, biotite, muscovite, ghosted orthopyroxene and opaques are interstitial to or interlocking with the quartz. Ghosted opaques (altered to hematite) are interstitial to the quartz and silicate minerals. Trace amounts of pyrite and pyrrhotite are preserved as inclusions within quartz and silicate minerals. A single grain of gold (ultra fine grained) occurs as an inclusions within hornblende (intergrown with quartz). The gold bearing hornblende is intergrown with ghosted orthopyroxene.

COMMENTS

The metamorphic wallrock replacement assemblage is representative of proximal (pyroxene hornfels) thermal metamorphism. There appears to be a clear genetic link between metamorphic wallrock replacement mineralogy and accessory quartz vein mineralogy. Native gold is associated with the dominant metamorphic wallrock replacement assemblage. Thermal metamorphism and metasomatism were synchronous, or metamorphism post-dated metasomatism. The nature of the late clay mineral (after orthopyroxene) is unresolvable.

Plate right. A single ultra fine grained gold inclusion within hornblende. 120 μm. rl/ppl.

SAMPLE NUMBER: 26005.1b

LOCATION: Bunkers ore zone

ROCK NAME: Metamorphosed quartz vein and metasedimentary wallrock

FIELD DESCRIPTION: A quartz veined metasedimentary rock from ore zone

OFFCUT DESCRIPTION:

The rock is a medium to dark grey, quartz veined, metasedimentary rock. Vitreous dark grey quartz is hosted by medium grey metasedimentary rock in which a primary lamination is preserved by metamorphic minerals. The vein is parallel to the relict lamination.

THIN SECTION DESCRIPTION

LITHOLOGY: PRIMARY MINERALOGY, TEXTURES

The distribution and grain-size variation of metamorphic replacement minerals preserves the primary bedding/lamination structure. The variation in metamorphic replacement mineralogy suggests that laminae of siltstone were interposed with laminae of mudstone.

ALTERATION

REPLACEMENT

Replacement of the sedimentary detrital assemblage is complete. The replacement assemblage comprises clinopyroxene, green-brown amphibole, brown biotite, garnet, muscovite, plagioclase (sodic to calcic), quartz, muscovite and pyrite. Laminae replaced predominantly by biotite are interposed with laminae replaced by interlocking equigranular plagioclase, green-brown biotite, and clinopyroxene and less abundant quartz. Trace amounts of pyrite, rutile and pyrrhotite are interstitial to the secondary silicate minerals. Coarser grains of garnet poikilitically enclose grains of plagioclase, quartz, biotite, amphibole and clinopyroxene.

In some parts of the rock (along late-stage microfractures) biotite is altered to late clay minerals (smectite and kaolin clays).

DEPOSITION

Early fractures are filled with fine to medium grained, tabular (granoblastic to porphyroclastic) quartz. The quartz has undulatory extinction and in some places appears to be attenuated. Very fine-grained green-brown amphibole, brown biotite and clinopyroxene are interstitial to or as inclusions within the quartz. Secondary fluid inclusions present comprise co-existing populations of aqueous liquid-rich types and gas-rich types.

Grains of anhedral pyrrhotite, some intergrown with chalcopyrite and pyrite are interstitial to the framework vein quartz occupying the same paragenetic position to amphibole and clinopyroxene. Chalcopyrite is locally altered to chalcocite.

COMMENTS

The metamorphic replacement assemblage is representative of pyroxene hornfels type metamorphism. Minerals common to quartz vein assemblages and wallrock replacement, including amphibole, pyrrhotite and clinopyroxene, suggest hydrothermal fluids were in equilibrium with wallrock or had been simultaneously thermally overprinted. Possible BiTeS minerals are intergrown with pyrrhotite.

Pale yellow Bi mineral (tetradymite) enclosed by pyrrhotite interstitial to framework vein quartz.

SAMPLE NUMBER: 26005.2a

LOCATION: Quorn ore zone

ROCK NAME: Quartz veined thermally metamorphosed sediment.

FIELD DESCRIPTION: A quartz vein host to metasedimentary wallrock fragments.

OFFCUT DESCRIPTION:

The samples is of smoky grey quartz vein material dispersed with grains of amphibole and dark grey to black, silt to sand-sized wallrock fragments.

THIN SECTION DESCRIPTION

LITHOLOGY: PRIMARY MINERALOGY, TEXTURES

Wallrock fragments have metamorphic replacement mineralogy and textures. The primary wallrock lithologies are not readily resolvable, however some crude relict lamination/bedding structures present are suggestive of a former sedimentary rock.

ALTERATION

REPLACEMENT

Metamorphic replacement of the primary wallrock lithology is complete. Replacement minerals comprise abundant tabular clinopyroxene and tabular to prismatic green-brown-blue amphibole. In many places the amphibole occurs interstitial to clinopyroxene together with anhedral fine grained quartz. Less abundant grains of tabular, anhedral orthopyroxene (altered to secondary Fe-oxides) are present. The orthopyroxene is overgrown by and altered to amphibole. Grains of sphene intergrown with ilmenite are present.

DEPOSITION

Angular, silt to sand-sized metamorphosed wallrock fragments are enclosed by an assemblage of voluminous fine to medium grained, tabular, anhedral quartz. At the interface of wallrock fragment-quartz cement, anhedral to subhedral grains of green-brown-blue amphibole and clinopyroxene are intergrown/interlocking with the quartz. Amphibole is intergrown with quartz away from wallrock-vein interfaces. Grains of sphene are interstitial to the quartz. Fluid inclusions hosted by quartz are mainly gas-rich types co-existing with less abundant aqueous liquid-rich types.

Trace amounts of ilmenite and arsentiferous pyrite are interstitial to or as inclusions within the quartz.

Late microfractures are filled with zeolite minerals that are locally intergrown with ultra fine-grained pyrite. Trace amounts of pyrrhotite are intergrown with arsentiferous pyrite (as inclusions within quartz).

Late-stage microfractures are filled with an Fe-oxide and/or Fe-bearing smectite mineral (the same as that replacing orthopyroxene).

COMMENTS

The metamorphic replacement assemblage comprising amphibole, clinopyroxene and orthopyroxene is best interpreted in terms of proximal thermal metamorphism; pyroxene hornfels would be an appropriate classification. The quartz veining includes hornblende and clinopyroxene (as differentiated from "accidental" wallrock material) indicating hydrothermal fluids were synchronous with or overprinted by peak metamorphism.

Plate right. Coexisting gas-rich and aqueous liquid-rich inclusions within quartz of the vein assemblage. 120 μm. ppl.

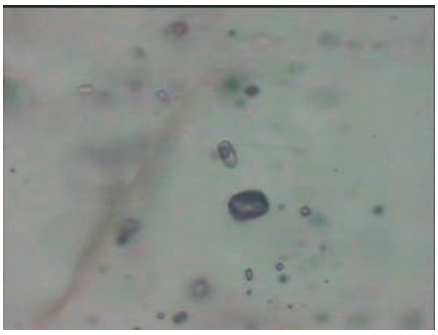

SAMPLE NUMBER: 26005.2b
LOCATION: Quorn ore zone
ROCK NAME: Quartz veined thermally metamorphosed sediment.

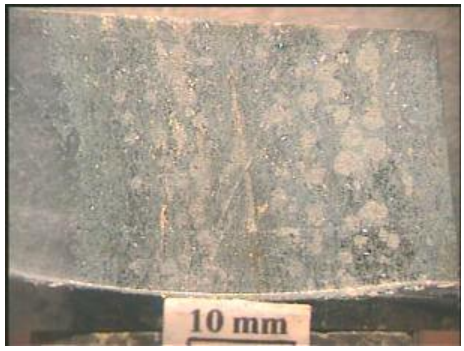

FIELD DESCRIPTION: A quartz veined metasedimentary rock

OFFCUT DESCRIPTION:

A dark grey to green-grey, unoxidised/unweathered, quartz veined metasedimentary rock. Dark grey vitreous quartz veins have formed parallel to ghosted lamination/bedding and cleavage within the green-grey metasedimentary wallrock. Abundant garnet porphyroblasts lie along the ghosted laminations/bedding and cleavage.

THIN SECTION DESCRIPTION

LITHOLOGY: PRIMARY MINERALOGY, TEXTURES

The grain-size variation and distribution of metamorphic replacement minerals defines a primary lamination/bedding structure. The grain-size variation within the metamorphic replacement assemblage may be interpreted in terms of interbedded mudstones and silty mudstones.

ALTERATION

REPLACEMENT

Replacement is complete. Replacement is dominated by mainly fine-grained green-brown-blue amphibole. Minor amounts of brown biotite, sphene, ilmenite, rutile, pyrrhotite and pyrite are interlocking with or interstitial to the amphibole. Anhedral grains of chalcopyrite and sphalerite are intergrown with pyrite and pyrrhotite. Pyrite is strongly pitted and etched in most places. Some (formerly Fe-rich) laminae are defined by concentrations of pyrite. Abundant, relatively coarse grained, porphyroblasts of garnet are present, typically lying along the boundaries between former laminae. Many of the euhedral garnet grains poikilitically enclose finer grained pyrite, magnetite, ilmenite, amphibole, biotite and sphene. Biotite is locally concentrated about the garnet porphyroblasts.

DEPOSITION

Microfractures within hornblende are filled with pyrrhotite, chalcopyrite and pyrite.

More voluminous fracturing is filled with fine to medium grained, anhedral, tabular quartz. The quartz has widespread undulatory extinction and locally porphyroclastic textures. The quartz is interlocking with grains and stringers of fine grained, tabular to prismatic green-blue amphibole (particularly at wallrock margins). Trace amounts of anhedral, fine-grained carbonate are interstitial to the quartz.

Trace amounts of molybdenite are interstitial to the quartz and hornblende. The molybdenite occurs in close proximity to generations of co-existing aqueous liquid-rich and gas-rich fluid inclusions. Some of the aqueous liquid-rich inclusions contain daughter halite crystals.

COMMENTS

Biotite and green-blue amphibole are common to the metamorphic replacement assemblage and quartz vein assemblages. Molybdenite contained within the quartz vein appears to be genetically related to saline fluid inclusions and gas-bearing fluid inclusions.

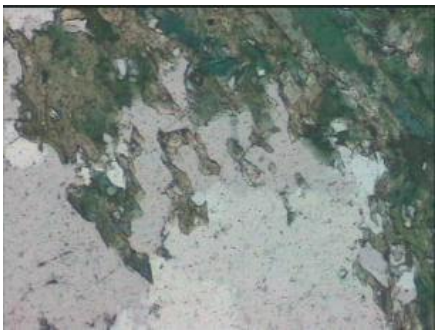

Plate right. Hornblende pervasive after the wallrock and also interlocking with quartz within the veining present. 1200 μm. ppl.

SAMPLE NUMBER: 26005.3
LOCATION: Ore zone within Magpie Schist
ROCK NAME: Thermally metamorphosed and metasomatised quartz veined sediments
FIELD DESCRIPTION: A quartz + feldspar veined metasediment.

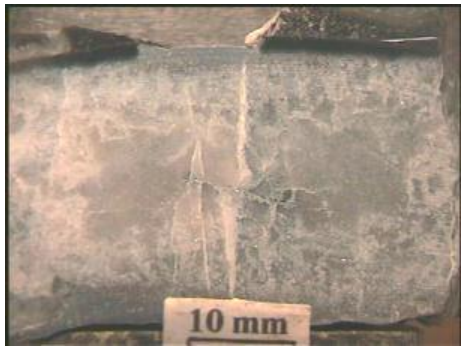

OFFCUT DESCRIPTION:

A dark grey to black, unoxidised/unweathered, mica-rich, metasedimentary rock is host to mottled pale to medium, vitreous grey quartz veining. The mottled colouration within the quartz veining is due to the present of domains of feldspar.

THIN SECTION DESCRIPTION

LITHOLOGY: PRIMARY MINERALOGY, TEXTURES

The variation in grain-size of the metamorphic replacement assemblages defines a crude lamination indicative of a former sedimentary rock.

ALTERATION

REPLACEMENT

Metamorphic replacement is complete. Replacement minerals comprise chlorite, biotite, muscovite, and rutile and trace amounts of ilmenite and pyrite. Decussate textured platy chlorite and muscovite dominate replacement. In most places, coarser grained tabular plates of muscovite occur as fine-grained porphyroblasts. Aggregates of rutile have a porphyroblastic distribution. Present amongst the pervasive chlorite are minor amounts of brown biotite. The brown biotite where present is partly to almost completely altered to chlorite, to suggest that all chlorite is a retrograde replacement of originally pervasive biotite. Trace amounts of ultra fine-grained pyrite are interstitial to the secondary silicate replacement or as inclusions within or intergrowth with rutile. Grains of apatite (and possibly other phosphorous minerals) are dispersed throughout the metamorphic mica assemblage. Chlorite (or chlorite after biotite) has a weak preferred orientation.

DEPOSITION

Voluminous fracturing of the metamorphic rock is filled mainly with fine to medium grained, anhedral tabular quartz, locally granoblastic to porphyroclastic in texture. Less abundant grains of alkali feldspar (albite and orthoclase), of similar grain-size, are interlocking with the quartz. Grains of biotite and muscovite occur as inclusions within quartz or interstitial to the quartz. Muscovite and biotite are poikilitically enclosed by alkali feldspar, and finer grained muscovite appears to replace alkali feldspar in places. Alkali feldspar and biotite occurring as intergrowths are concentrated along vein-wallrock interfaces, or occur as irregular "stringers" within the voluminous quartz assemblage. Central parts of the vein geometry are occupied almost exclusively by quartz. The biotite is locally altered to chlorite and alkali feldspar to illitic clay and carbonate. Some coarse-grained alkali feldspar is interlocking with quartz at some wallrock-vein interfaces. Grains of apatite occur as inclusions within the quartz. Co-existing gas-rich and aqueous liquid rich inclusions are present.

Grains of rutile, pyrrhotite, pyrite, sphalerite, galena and chalcopyrite are interstitial to or as inclusions within the quartz but mainly silicate minerals (feldspars and micas), in places directly overgrown by (and apparently intergrown with) anhedral carbonate minerals. Possible tetradymite is intergrown with pyrrhotite.

Native gold is locally concentrated as multiple anhedral to euhedral grains interstitial to or as inclusions within quartz, alkali feldspar, biotite and muscovite where the later silicate minerals are concentrated (i.e. stringers or at wallrock-vein interfaces). The gold is intergrown with rutile. Most of the gold in fact occurs as inclusions in alkali feldspar (together with fine-grained muscovite). Minor amounts of pyrrhotite occupy the same paragenetic position and is intergrown with native gold. Some gold fills microfractures in alkali feldspar.

Late microfracturing transecting both quartz-feldspar-biotite veining and wallrock are filled with fine to very fine-grained carbonate and pyrite. In other places the carbonate is interstitial to quartz, feldspar and biotite.

COMMENTS

Alkali feldspar comprising albite and orthoclase is dominant in the vein assemblage. Native gold, associated with rutile and pyrrhotite, is concentrated with and closely associated alkali feldspar (and mica minerals). The quartz veining fractures preferentially along the stringers of alkali feldspar thus exposing gold on fracture surfaces. Galena occupies the same paragenetic position as gold (inclusions in K-spar).

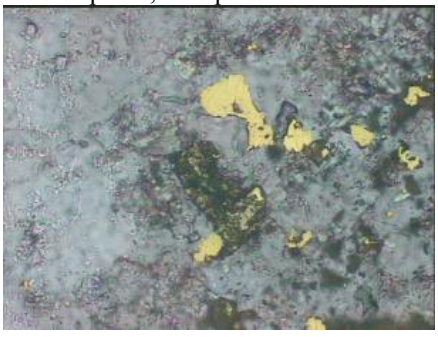

Plate right. Native gold as intergrowths with and inclusions within alkali feldspar, quartz and pyrrhotite. 300 μm.

SAMPLE NUMBER: 26005.4
LOCATION: Magpie schist
ROCK NAME: Quartz veined, metamorphosed sediment
FIELD DESCRIPTION: A quartz veined, metasedimentary rock

OFFCUT DESCRIPTION:

A mottled pale to dark smoky grey, vitreous quartz vein is hosted by a dark grey to black, unoxidised/unweathered metamorphic rock. Fine grained mica minerals define a penetrative fissility within the rock. Biotite and feldspar are present within the quartz veining.

THIN SECTION DESCRIPTION

LITHOLOGY: PRIMARY MINERALOGY, TEXTURES

The distribution and grain-size variation of a metamorphic replacement assemblage preserves a primary lamination/bedding of a former fine-grained sedimentary rock. Ghosted/relict silt-sized detrital fragments are present in the more voluminous laminae.

ALTERATION

REPLACEMENT

Metamorphic replacement is complete. Recrystallised (silt-sized) detrital quartz is intergrown with platy chlorite. The chlorite has a sub-preferred orientation defining a penetrative strain fabric within the rock. Coarser grained play biotite and aggregates of platy biotite are dispersed about the chlorite, defining porphyroblasts and porphyroblastic aggregates. Some amounts of muscovite also occur as randomly orientated porphyroblasts. Grains and aggregates of rutile and ilmenite are dispersed about the silicate replacement assemblage. In some places these aggregates of rutile and ilmenite together with biotite form porphyroblastic aggregates. Some laminae are replaced almost exclusively by platy brown biotite with only minor amounts of finer grained chlorite interstitial to the biotite.

DEPOSITION

Voluminous fracturing of the metamorphic wallrock is filled mainly with fine to medium grained, anhedral, tabular quartz, locally granoblastic to porphyroclastic in texture. The quartz is interlocking with alkali feldspar (K-feldspar and albite), biotite and muscovite mainly at or proximal to wallrock-vein interfaces. The muscovite typically occurs as inclusions within or as a replacement of alkali feldspar. Minor amounts of carbonate form an overprint to the alkali feldspar, or have formed interstitially to quartz, biotite and muscovite. Some coarse-grained alkali feldspar occurs at bends within the vein-wallrock interface. Grains of apatite occur as inclusions within quartz. Earliest secondary fluid inclusions comprise gas-rich types coexisting with aqueous liquid-rich types.

Grains and aggregates of anhedral pyrrhotite and rutile are interstitial to and interlocking with quartz and silicate minerals. Sphalerite, chalcopyrite and trace amounts of galena and possible BiTeS minerals are intergrown with or occupy the same paragenetic position as pyrrhotite and rutile.

Later microfracturing is filled with fine to very fine-grained carbonate. The carbonate also occurs interstitially to the silicate minerals or as late secondary inclusions within quartz.

COMMENTS

A metamorphosed silty mudstone. A greater abundance of preserved and partly altered biotite within the wallrock lends support to the interpretation that some of the chlorite present in the wallrock is a retrograde alteration of biotite. Biotite occurs predominantly as micro-porphyroblasts together with muscovite whereas chlorite is abundant in the "matrix" and is representative of early replacement.

Plate right. Biotite micro-porphyroblasts in wallrock and biotite intergrown with alkali feldspar and quartz within the vein at the wallrock-vein interface. 1200 μm.

SAMPLE NUMBER: 26005.5

LOCATION: Magpie schist

ROCK NAME: Quartz-feldspar-biotite vein

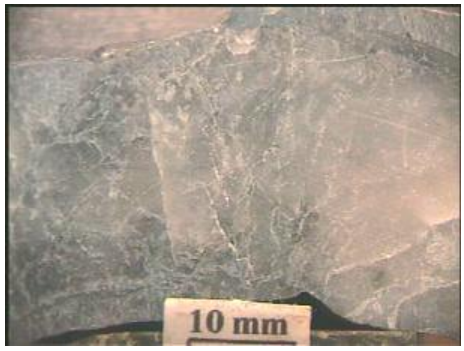

FIELD DESCRIPTION: Mineralised quartz vein

OFFCUT DESCRIPTION:

The sample is of grey to smoky grey, unweathered/unoxidised, vitreous quartz vein attached to which are minor amounts of dark grey metasedimentary wallrock. The quartz vein and wallrock are traversed by late carbonate veinlets.

THIN SECTION DESCRIPTION

LITHOLOGY: PRIMARY MINERALOGY, TEXTURES

Primary wallrock textures and composition are unresolvable.

ALTERATION

REPLACEMENT

Metamorphic replacement of the wallrock is complete. Replacement is dominated by fine-grained muscovite intergrown with platy chlorite and dispersed with platy, coarser grained biotite and aggregates of biotite. Minor amounts of quartz are interstitial to the muscovite and chlorite. Biotite is partly altered to chlorite in most places. Grains of rutile and ilmenite are interstitial to the silicate minerals.

DEPOSITION

The vein assemblage comprises abundant fine to medium grained, anhedral, tabular quartz, locally granoblastic to porphyroclastic in texture. The quartz has widespread undulatory extinction. Grains and aggregates of alkali feldspar (albite and orthoclase) are interlocking with the quartz. The alkali feldspar is host to inclusions of platy muscovite and less abundant biotite. The muscovite inclusions are commonly arranged in a radiating form. Biotite and muscovite also occur interstitially to and as inclusions within the quartz. Plates and aggregates of biotite occur along stringers within the quartz veining. Much of the biotite is altered to platy chlorite. The quartz is interlocking with apatite, and is host to inclusions of apatite and xenotime. Whereas chlorite has formed after biotite, significant amounts of fine to very fine-grained carbonate have formed after muscovite and alkali feldspar.

Grains of rutile are intergrown with or enclosed by biotite (→ chlorite). Minor amounts of pyrrhotite occur as inclusions within or are interstitial to the silicate minerals.

Late microfractures are filled with carbonate, and carbonate also occurs interstitially to quartz, or appears to flood some areas forming interstitially to quartz grains over a wide area.

COMMENTS

A metamorphosed mudstone wallrock as evidenced by the abundance of muscovite, chlorite and biotite. Only minor amounts of pyrrhotite are present within the vein assemblage, which contains significant amounts of alkali feldspar and muscovite.

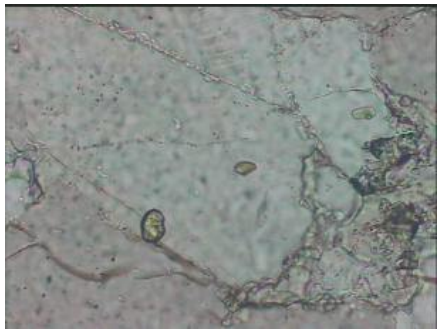

Plate right. Xenotime and biotite inclusions within quartz. 300 μm. ppl.

SAMPLE NUMBER: 26005.6
LOCATION: Lower Blake Beds
ROCK NAME: Metamorphosed, quartz veined meta-mudstone

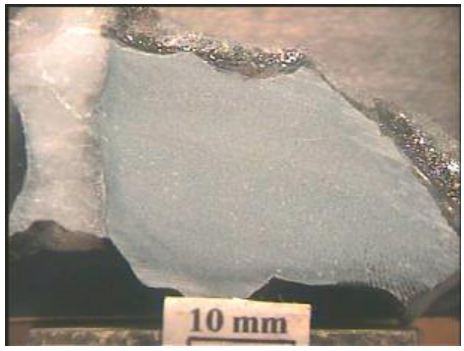

FIELD DESCRIPTION: Quartz veined metasediment

OFFCUT DESCRIPTION:

A dark grey to green-grey, unoxidised/unweathered, quartz veined metasedimentary rock. Quartz veining is smoky grey, vitreous in appearance and includes alkali feldspar and biotite concentrated along wallrock margins.

THIN SECTION DESCRIPTION

LITHOLOGY: PRIMARY MINERALOGY, TEXTURES

The distribution and grain-size variation of metamorphic replacement minerals preserves a primary lamination/bedding. Within some laminae, metamorphic replacement mica minerals enclose ghosted, silt-sized detrital framework clasts.

ALTERATION

REPLACEMENT

Metamorphic and metasomatic replacement is complete. Fine-grained platy chlorite and brown biotite dominate replacement, the later locally altered to chlorite. How much of the chlorite is a replacement of biotite is unresolvable. The chlorite and biotite are intergrown with very fine to ultra fine-grained quartz, much of which is recrystallised detrital quartz. Biotite is aggregated in some places, defining spots. Ghosted tabular cubic to rhombohedral porphyroblasts present are altered to quartz poikilitically enclosing platy biotite and chlorite. Less abundant fine to very fine-grained muscovite is intergrown with the chlorite, biotite and quartz. Biotite and muscovite are more abundant in some laminae. Similarly quartz is more abundant in some laminae reflecting primary compositional variation across laminae. Grains and aggregates of rutile and ilmenite are dispersed about the secondary silicate assemblage, some of the coarser grained examples poikilitically enclosing biotite, muscovite and quartz. Sparse grains of pyrite/As-pyrite are also dispersed about the secondary assemblage. Biotite is most strongly retrograded to chlorite along shears proximal to quartz vein margins.

DEPOSITION

Fractures mainly at high angles to ghosted lamination are filled with fine grained, anhedral, tabular quartz locally granoblastic and porphyroclastic in texture. Plates/grains and aggregates of brown biotite (locally altered to chlorite) and alkali feldspar (locally altered to illite and carbonate) are interlocking with and/or interstitial to the quartz. The biotite and alkali feldspar are concentrated along the wallrock-vein interface or along stringers leading from the wallrock-vein interface. Apatite is present as inclusions within and intergrowths with quartz, whereas very fine to ultra fine grained xenotime occurs as inclusions within quartz. Fluid inclusions in quartz comprise secondary/pseudo-secondary, co-existing gas-rich and aqueous liquid-rich types.

Grains of ultra fine-grained rutile, pyrite/As-pyrite and chalcopyrite are interstitial to or as inclusions within quartz, alkali feldspar and quartz. Native gold, intergrown with minor amounts of rutile, is enclosed by brown biotite and alkali feldspar at the vein-wallrock interface. Galena and possible ultra fine-grained BiTeS minerals (with distinct acicular/prismatic morphologies) are present as inclusions (together with co-existing gas-rich inclusions) in quartz in other parts of the vein occupying the same paragenetic position as gold.

Late microfractures (cutting wallrock and quartz + feldspar + biotite veining) are filled with very fine-grained carbonate. Carbonate has also formed interstitially to quartz and as late secondary inclusions within quartz.

COMMENTS

Gold occurs as intergrowths with brown biotite, alkali feldspar (→ carbonate and illite) and quartz close to the vein-wallrock interface. Galena is present, although not intergrown with gold and occupying the same paragenetic position in other parts of the vein. Very similar overall paragenesis to the Western Tanami.

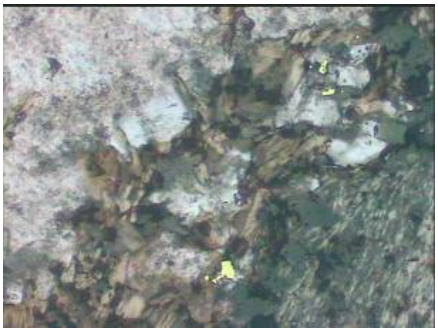

Plate right. Native gold intergrown with biotite and alkali feldspar at wallrock-vein interface. 600 μm.

SAMPLE NUMBER: 26005.07
LOCATION: "ore zone" ?western wall, Windy Hill open pit
ROCK NAME: Recrystallised "mesothermal" style quartz vein hosted by metasediment
FIELD DESCRIPTION: Oxidised quartz vein

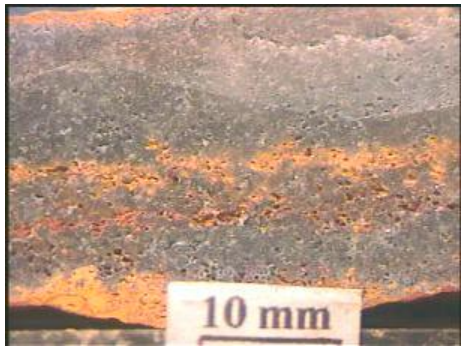

OFFCUT DESCRIPTION:

The sample comprises a partly/locally oxidised/weathered, vitreous grey quartz vein. Banding within the quartz vein is highlighted or preserved by the distribution of secondary hydrated Fe-oxides. A sugary or granoblastic texture is evident within the quartz vein. The vein margin is parallel to a leached/weathered wallrock (not present).

THIN SECTION DESCRIPTION

LITHOLOGY: PRIMARY MINERALOGY, TEXTURES

Ghosted silt to fine sand-sized wallrock fragments are enclosed within the vein assemblage (marginal to where the wallrock once existed). The wallrock fragments have poorly preserved primary fragmental textures.

ALTERATION

REPLACEMENT

Replacement of the wallrock fragments is complete. Interlocking, granoblastic quartz and mica minerals, including muscovite and ghosted biotite dominate replacement. Ghosted Al-silicates or feldspars are also present. Biotite is altered to hydrated Fe-oxides and hematite. Ultra fine-grained hydrated Fe-oxides form a dusting over the secondary silicate assemblage.

DEPOSITION

The vein assemblage is composed mainly of fine grained, tabular, anhedral quartz. Granoblastic textures pervade the vein lithology, with triple-point grain boundaries ubiquitous. Grains of relict apatite are interlocking with the quartz. Abundant ghosted/leached opaques (sulphide minerals) are interlocking with the quartz. Grains and aggregates of a tabular to prismatic green amphibole occur as inclusions within the anhedral quartz. Partly preserved sulphide minerals occur as inclusions within or interstitial to the quartz, some intergrown with the amphibole mineral. Ultra fine-grained rutile and pyrrhotite occur as inclusions within the quartz.

Sparsely preserved, secondary/pseudosecondary fluid inclusions predating recrystallisation of quartz comprise mainly gas-rich/filled types co-existing with aqueous gas-bearing liquid-rich inclusions. Gases present are interpreted to include CO_2. More abundant secondary fluid inclusions post-dating recrystallisation comprise co-existing gas-rich/filled and aqueous liquid-rich types.

Cavities resulting from leaching of opaques/sulphide minerals are lined or sealed with fine to very fine grained tabular to prismatic hematite and hydrated Fe-oxides.

COMMENTS

The vein lithology is hosted by metamorphosed sedimentary rock. The primary quartz vein assemblage, comprising mostly quartz, is recrystallised, resulting in the granoblastic texture now preserved. The aggregates of very fine to ultra fine-grained amphibole are part of the recrystallisation assemblage. Apatite has not recrystallised and is in some places deformed in a brittle manner.

Plate right. Aggregates of secondary amphibole occurring as inclusions within the recrystallised vein quartz. 600 μm. ppl.

SAMPLE NUMBER: 26005.08
LOCATION: Ore zone ?eastern wall, Windy Hill open pit
ROCK NAME: Recrystallised, quartz veined, meta-sedimentary rock
FIELD DESCRIPTION: Quartz veined metasedimentary rock

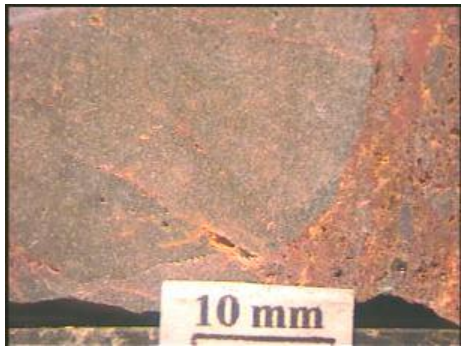

OFFCUT DESCRIPTION:

The sample is of weathered/oxidised, translucent to vitreous grey, quartz vein hosted by red-brown, weathered/oxidised fine grained metamorphosed sedimentary wallrock. Residual cavities within the oxidised/weathered wallrock are partly/completely filled with hydrated Fe-oxides.

THIN SECTION DESCRIPTION

LITHOLOGY: PRIMARY MINERALOGY, TEXTURES

Wallrock has a relict fragmental texture. The distribution and grain-size variation of mainly tabular secondary/replacement minerals defines the former fragmental texture. The distribution and grain-size variation of secondary minerals also define former lamination structures.

ALTERATION

REPLACEMENT

Replacement of the primary rock type is complete. Replacement is dominated by granoblastic quartz interlocking with equally abundant platy (ghosted) biotite. Trace amounts of muscovite are present, and possibly some amounts of ghosted feldspar and/or Al-silicates are also present. Hydrated Fe-oxides and smectite/kaolin clays have formed after biotite and possible Al-silicate/feldspar minerals.

DEPOSITION

Fractures formed parallel to the bedding within the host rock are filled mainly with equigranular, tabular quartz. The quartz has a mainly granoblastic texture with some porphyroclastic domains in some places. The quartz is host to ultra fine to very fine-grained inclusions of muscovite, biotite, pyrrhotite, pyrite and rutile. The inclusions of biotite, rutile, pyrrhotite and muscovite, together with possible ultra fine-grained amphibole and tourmaline are more abundant within the domains of granoblastic quartz. Ghosted/leached opaque/sulphide minerals are interlocking with the granoblastic quartz.

More abundant fluid inclusions preserved within relatively coarse-grained quartz porphyroclasts comprise abundant gas-rich/filled types co-existing with less abundant aqueous liquid-rich types. Fluid inclusions contained within the finer grained granoblastic quartz are less abundant but also comprise more abundant gas-rich/filled types co-existing with less abundant aqueous liquid-rich types.

Residual cavities are lined with hydrated Fe-oxides and hematite.

COMMENTS

The quartz vein is parallel to relict bedding plane structures within the meta-sedimentary wallrock. The granoblastic vein quartz plus inclusions is representative of recrystallisation of primary quartz + silicate + sulphide vein assemblage. The abundant biotite, muscovite, pyrrhotite, rutile, amphibole and tourmaline inclusions are part of that recrystallisation assemblage. Relatively fluid inclusion rich quartz porphyroclasts are relict members of the primary quartz vein lithology.

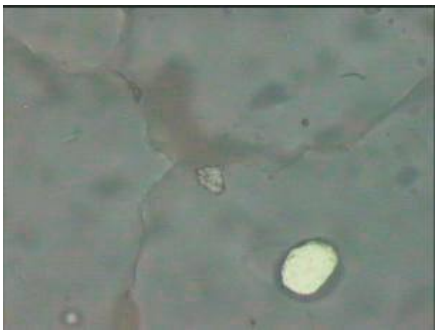

Plate right. Pyrrhotite and possible BiTeS mineral inclusions within granoblastic quartz. 120 μm. rl/ppl.

SAMPLE NUMBER: 26005.09a and b
LOCATION: Groundrush open pit
ROCK NAME: Gold bearing quartz vein breccia
FIELD DESCRIPTION: Gold bearing quartz vein breccia

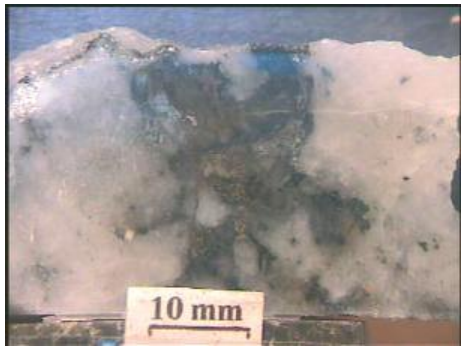

OFFCUT DESCRIPTION:

The sample comprises a fragment of massive translucent to grey vitreous quartz vein material. The quartz is host to irregularly shaped, deformed, metasomatised sand to cobble-sized wallrock fragments. Biotite and chlorite are present with the wallrock replacement assemblage.

THIN SECTION DESCRIPTION

LITHOLOGY: PRIMARY MINERALOGY, TEXTURES

The wallrock fragments have very poorly preserved primary doleritic texture. In some places the distribution of secondary minerals defines former interlocking pyroxene and plagioclase. Equally ghosted former Fe/Ti-oxides are interstitial to the ghosted silicate framework assemblage. Trace amounts of relict interstitial (recrystallised) quartz are present. Prior to alteration of any stage, the doleritic textured lithology was moderately to strongly deformed. The lithology was fragmented and comminuted along penetrative shears and fractures.

ALTERATION

REPLACEMENT

Replacement of the sheared and deformed primary igneous lithology is complete. An early replacement assemblage comprises relict to partly preserved green-brown-blue amphibole intergrown with ghosted plagioclase/albite. Grains and aggregates of rutile, ilmenite and sphene are dispersed about the amphibole and plagioclase replacement assemblage, and concentrated after former primary Fe/Ti-oxides.

The early replacement assemblage merges with and is overprinted by pervasive platy brown biotite that is intergrown with the early and a second generation of more acicular, clear to green coloured amphibole (anthophyllite). The brown biotite is also locally intergrown with K-feldspar (orthoclase). Grains and aggregates of rutile are part of the second stage replacement assemblage.

Chlorite has formed after biotite and sericite/illite has formed after plagioclase/albite in some parts of the wallrock. Fine to medium grained carbonate, intergrown with chlorite, overprints the early silicate replacement.

In some parts of the wallrock grains and aggregates of native gold are enclosed by or intergrown with the brown biotite, K-feldspar and second-stage amphibole (anthophyllite). In these locations the native gold typically forms overgrowths to sphene, ilmenite and rutile and in some cases also the early amphibole. Some gold occurs as inclusions within K-feldspar, biotite and amphibole. Trace amounts of chalcopyrite and arsentiferous pyrite occupy the same paragenetic position. Late carbonate also forms an overprint to the gold.

DEPOSITION

The wallrock fragments are enclosed by voluminous fine grained, anhedral, tabular quartz. The quartz has widespread undulatory extinction, sub-grain boundary development and crenulate grain boundaries. The wallrock at wallrock-quartz vein boundaries is mantled by radiating aggregates of acicular amphibole (anthophyllite) much of which occurs as ultra fine-grained inclusions within quartz directly adjacent to wallrock. The amphibole is locally overprinted by carbonate. Grains and aggregates of biotite (→ chlorite) and K-feldspar are interlocking with the quartz and amphibole. Carbonate has formed interstitially to quartz and forms overgrowths to biotite and amphibole in places. The deformed quartz is host to relict populations of mainly gas-rich/filled inclusions co-existing with aqueous liquid-rich inclusions. Relatively coarse grained pyrite and arsentiferous pyrite are interlocking with the quartz. Some recrystallised quartz is intergrown with biotite, K-feldspar and amphibole. Chalcopyrite is present. One grains of gold intergrown with biotite (→ chlorite) is interstitial to quartz and overprinted by carbonate. Carbonate and pyrite fill late fractures.

COMMENTS

There is a strong gold association with K-feldspar + biotite + amphibole + Ti-oxide metasomatism within the wallrock. A gold quartz vein association is also present. Arsentiferous pyrite is present in the wallrock and vein assemblage, however there is no close spatial association with gold. Pyrite and chalcopyrite are associated with the carbonate overprint.

Plate right. Gold intergrown with K-feldspar (after plagioclase), amphibole and biotite. 600 μm. rl/ppl.

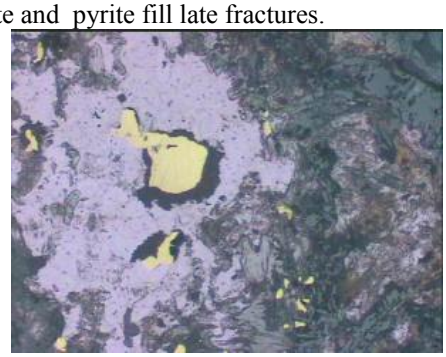

APPENDIX TWO:

ELECTRON MICROPROBE ANALYSIS OF GOLD AND SULPHIDE GRAINS

GOLD & SULPHIDE CHEMISTRY

Location	Lower Blake Beds, ore zone (26005.06)					Magpie schist, ore zone (26005.03)						Magpie
Paragen.	Gold grains enclosed by biotite at quartz vein margin.			Galena interstitial to recrystallised quartz.		Galena interstitial to quartz and biotite.		Gold intergrown with K-feldspar, biotite and muscovite		Galena in K-spar, quartz and pyrrhotite		Galena in biotite
Weight%	6.1 a	6.1 b	6.1 c	6.2a	6.2b	3.2 a	3.2 b	3.3a	3.3b	3.1a	3.1b	4.1a
S				16.01	12.82	13.49	10.57	0.01	0.01	12.24	12.97	12.76
Fe	0.12	0.42	0.38	0.00	0.04	0.08	0.03	0.04	0.00	0.17	0.01	0.25
Cu	0.04	0.12	0.05	0.02	0.05							
As				34.74								
Mo												
Ag	6.54	7.27	6.43	0.10	0.20	0.20	0.26	8.46	8.78	0.09	0.12	0.06
Sb				0.00	0.00							
Te				0.00	0.00	0.03	0.00	0.00	0.02	0.02	0.00	0.03
Au	94.01	91.73	92.39	0.00	0.00	0.00	0.20	90.98	90.52	0.00	0.00	0.00
Pb	0.00	0.00	0.00	90.64	84.31	86.71	70.40	0.00	0.00	78.48	87.44	88.64
Bi	0.53	0.58	0.71	0.56	0.68	0.47	0.28	0.64	0.45	0.08	0.29	0.18
TOTAL	101.24	100.11	99.96	142.08	98.09	100.97	81.73	100.12	99.79	91.09	100.83	101.92
Atomic %												
S						49.79	48.86	0.04	0.08	49.90	48.78	47.83
Fe						0.17	0.07	0.13	0.00	0.40	0.03	0.54
Cu												
As												
Mo												
Ag						0.22	0.35	14.42	14.99	0.11	0.13	0.06
Sb												
Te						0.03	0.00	0.00	0.03	0.02	0.00	0.03
Au						0.00	0.15	84.85	84.51	0.00	0.00	0.00
Pb						49.53	50.37	0.00	0.00	49.52	50.89	51.43
Bi						0.26	0.20	0.56	0.40	0.05	0.17	0.10
TOTAL												
S				0.13	0.11	0.11	0.09	0.00	0.00	0.10	0.11	0.10
Fe	0.00	0.00	0.00	0.00	0.00	0.00	0.00	0.00	0.00	0.00	0.00	0.00
Cu	0.00	0.00	0.00	0.00	0.00							
As				0.15								
Mo												
Ag	0.05	0.05	0.05	0.00	0.00	0.00	0.00	0.06	0.06	0.00	0.00	0.00
Sb				0.00	0.00							
Te				0.00	0.00	0.00	0.00	0.00	0.00	0.00	0.00	0.00
Au	0.52	0.51	0.51	0.00	0.00	0.00	0.00	0.50	0.50	0.00	0.00	0.00
Pb	0.00	0.00	0.00	1.12	1.04	1.07	0.87	0.00	0.00	0.97	1.08	1.09
Bi	0.01	0.01	0.01	0.01	0.01	0.00	0.00	0.01	0.00	0.00	0.00	0.00

GOLD & SULPHIDE CHEMISTRY

Location	Groundrush ore zone (26005.09), pit floor					Windy Hill ore (26005.07)		DBS ore zone, DBD352/197.8m				
Paragen.	Gold grains intergrown with K-feldspar, biotite and quartz after wallrock fragment at quartz vein margin.					Opaque minerals in vein quartz		Gold and sulphide grains interstitial to locally recrystallised vein quartz.				
Weight %	9.1a	9.1b	9.1c	9.1d	9.1e	7.1a	7.1b	dbs.1a	dbs.2b	dbs.1c	dbs.1b	dbs.1d
S	0.05					0.06	17.85			36.61	49.38	29.07
Fe	0.03	0.05	0.01	0.10	0.05	40.71	0.45	0.00	0.05	49.19	44.19	50.53
Cu		0.00	0.03	0.05	0.03	0.04	2.79	0.05	0.08	0.89	0.21	0.02
As												0.09
Mo						0.00	0.21					
Ag	6.54	6.39	6.95	6.16	6.46	0.01	0.07	14.23	13.72	0.01	0.04	0.00
Sb												
Te	0.00	0.02	0.05	0.19	0.06	0.00	0.00			0.00	0.00	0.00
Au	92.68	92.84	93.18	92.84	93.16	0.06	0.00	69.73	75.82	0.00	0.00	0.12
Pb	0.00	0.00	0.00	0.00	0.00	0.01	0.06			0.00	0.02	
Bi	0.54	0.97	0.59	0.60	0.67	0.00	0.15	0.80	0.73	0.05	0.00	0.01
TOTAL	99.83	100.27	100.81	99.94	100.42	40.88	21.59	84.81	90.40	86.74	93.85	79.84
Atomic %												
S	0.16					0.24	90.89			56.06	65.95	49.99
Fe	0.10	0.17	0.03	0.34	0.17	99.62	1.32	0.00	0.18	43.24	33.89	49.89
Cu		0.01	0.10	0.14	0.09	0.08	7.16	0.17	0.26	0.69	0.14	0.02
As												0.07
Mo						0.00	0.36					
Ag	11.34	11.06	11.91	10.68	11.14	0.01	0.10	26.90	24.57	0.00	0.02	0.00
Sb												
Te	0.00	0.03	0.07	0.28	0.08	0.00	0.00			0.00	0.00	0.00
Au	87.93	87.87	87.37	88.03	87.93	0.04	0.00	72.15	74.32	0.00	0.00	0.03
Pb	0.00	0.00	0.00	0.00	0.00	0.01	0.05			0.00	0.00	
Bi	0.48	0.87	0.52	0.53	0.60	0.00	0.12	0.78	0.68	0.01	0.00	0.00
TOTAL												
S	0.00					0.00	0.15			0.30	0.41	0.24
Fe	0.00	0.00	0.00	0.00	0.00	0.27	0.00	0.00	0.00	0.33	0.29	0.33
Cu		0.00	0.00	0.00	0.00	0.00	0.01	0.00	0.00	0.00	0.00	0.00
As												0.00
Mo						0.00	0.00					
Ag	0.05	0.05	0.05	0.04	0.05	0.00	0.00	0.10	0.10	0.00	0.00	0.00
Sb												
Te	0.00	0.00	0.00	0.00	0.00	0.00	0.00			0.00	0.00	0.00
Au	0.51	0.51	0.52	0.51	0.52	0.00	0.00	0.39	0.42	0.00	0.00	0.00
Pb	0.00	0.00	0.00	0.00	0.00	0.00	0.00			0.00	0.00	
Bi	0.01	0.01	0.01	0.01	0.01	0.00	0.00	0.01	0.01	0.00	0.00	0.00

GOLD AND SULPHIDE CHEMISTRY

Location	Twin Bonanza (26021.03)					Twin Bonanza (26020.22)			Old Pirate (26023.01)			
Paragenesis	Electrum grain in arsenopyrite and galena and acicular boulangerite in quartz veinlets					Electrum and galena intergrown with carbonate, pyrite and quartz			Electrum, gold, chalcopyrite and galena intergrown with quartz, carbonate and biotite			
Minerals	Electrum		Galena & Boulangerite			Electrum & galena			Electrum and galena			
Wt %	a1	a2	b1	b2	b3	a1	a2	a3	a1	a2	a3	b1
S			11.77	14.07	11.88			14.04			10.38	
Fe	0.39	0.53	0.00	0.07	0.03	0.09	0.10	4.10	0.13	0.11	0.24	0.31
Cu	0.00	0.04	0.07	0.10	0.06	0.00	0.00	0.00	0.28	0.08	0.03	0.00
Ag	15.52	14.99	0.10	0.11	0.16	19.58	21.38	0.15	11.51	3.15	1.42	17.75
Sb	0.07	0.02	0.00	22.37	0.06	0.00	0.00	0.00	0.00	0.00	0.00	0.00
Te	0.00	0.07	0.04	0.00	0.02	0.00	0.03	0.02	0.13	0.00	0.00	0.11
Pt	0.00	0.00	0.00	0.00	0.00	0.00	0.00	0.00	0.00	0.00	0.00	0.00
Au	85.80	84.65	0.00	0.00	0.00	80.79	80.01	2.36	88.43	94.49	9.41	77.90
Hg	0.00	0.00	0.00	0.00	0.00	0.00	0.00	0.00	0.00	0.00	0.00	0.00
Pb	0.00	0.00	81.73	44.44	81.76	0.00	0.00	78.44	0.00	0.00	79.51	0.07
Bi	0.82	0.68	0.17	0.87	0.08	0.52	0.64	0.26	0.77	1.04	0.09	0.87
TOTAL	102.61	100.98	93.89	82.02	94.05	100.98	102.17	99.37	101.23	98.87	101.08	97.02
Atomic %												
S			48.01	51.94	48.17			48.41			41.85	
Fe	1.18	1.63	0.01	0.14	0.06	0.28	0.29	8.12	0.41	0.38	0.55	0.97
Cu	0.00	0.11	0.14	0.19	0.12	0.00	0.00	0.00	0.77	0.25	0.06	0.00
Ag	24.36	23.86	0.12	0.12	0.20	30.48	32.54	0.15	18.83	5.66	1.70	28.83
Sb	0.10	0.03	0.00	21.74	0.07	0.00	0.00	0.00	0.00	0.00	0.00	0.00
Te	0.00	0.09	0.04	0.00	0.02	0.00	0.04	0.02	0.17	0.00	0.00	0.16
Pt	0.00	0.00	0.00	0.00	0.00	0.00	0.00	0.00	0.00	0.00	0.00	0.00
Au	73.69	73.73	0.00	0.00	0.00	68.82	66.62	1.32	79.17	92.75	6.17	69.25
Hg	0.00	0.00	0.00	0.00	0.00	0.00	0.00	0.00	0.00	0.00	0.00	0.00
Pb	0.00	0.00	51.57	25.38	51.32	0.00	0.00	41.84	0.00	0.00	49.62	0.06
Bi	0.66	0.56	0.11	0.49	0.05	0.41	0.51	0.14	0.65	0.96	0.06	0.73
TOTAL	100.00	100.00	100.00	100.00	100.00	100.00	100.00	100.00	100.00	100.00	100.00	100.00
det. Limit.												
S			0.10	0.11	0.10			0.11			0.08	
Fe	0.00	0.00	0.00	0.00	0.00	0.00	0.00	0.03	0.00	0.00	0.00	0.00
Cu	0.00	0.00	0.00	0.00	0.00	0.00	0.00	0.00	0.00	0.00	0.00	0.00
Ag	0.11	0.11	0.00	0.00	0.00	0.14	0.15	0.00	0.08	0.02	0.01	0.13
Sb	0.00	0.00	0.00	0.13	0.00	0.00	0.00	0.00	0.00	0.00	0.00	0.00
Te	0.00	0.00	0.00	0.00	0.00	0.00	0.00	0.00	0.00	0.00	0.00	0.00
Pt	0.00	0.00	0.00	0.00	0.00	0.00	0.00	0.00	0.00	0.00	0.00	0.00
Au	0.48	0.48	0.00	0.00	0.00	0.46	0.45	0.01	0.50	0.53	0.05	0.44
Hg	0.00	0.00	0.00	0.00	0.00	0.00	0.00	0.00	0.00	0.00	0.00	0.00
Pb	0.00	0.00	0.99	0.54	0.99	0.00	0.00	0.95	0.00	0.00	0.96	0.00
Bi	0.01	0.01	0.00	0.01	0.00	0.01	0.01	0.00	0.01	0.01	0.00	0.01

APPENDIX THREE:

ELECTRON MICROPROBE ANALYSIS OF BIOTITE GRAINS

BIOTITE CHEMISTRY

Location	Lower Blake Beds, ore zone (26005.06)					Magpie Schist, ore zone (26005.03)				Magpie Schist, ore zone (26005.04)			
Paragen.	Biotite intergrown with quartz and K-spar at vein margin and enclosing gold.					Biotite intergrown with vein quartz and K-feldspar.				Biotite intergrown with vein quartz enclosing galena.			
weight%	6.1d	6.1e	6.1f	6.1f	6.1f	3.4 a	3.4 b	3.4 c	3.4 d	4.1b	4.1c	4.1c repeat	4.1c repeat
SiO2	33.50	34.69	35.91	35.91	35.91	35.18	33.27	33.37	32.83	33.81	31.58	28.65	32.85
TiO2	2.07	2.10	2.06	2.06	2.06	2.07	1.73	1.83	1.99	2.16	1.53	0.98	1.69
Al2O3	19.60	19.11	19.48	19.48	19.48	19.39	19.03	18.93	18.82	18.38	17.28	17.53	18.24
FeO	22.85	22.44	21.95	21.95	21.95	22.17	24.24	24.88	22.76	25.84	27.75	29.45	25.45
MnO	0.08	0.02	0.08	0.08	0.08	0.08	0.08	0.10	0.07	0.10	0.08	0.15	0.12
MgO	7.24	7.55	7.32	7.32	7.32	7.12	7.42	7.20	7.23	7.43	8.20	9.37	7.65
CaO	0.05	0.03	0.11	0.11	0.11	0.00	0.05	0.00	0.00	0.06	0.02	0.04	0.03
Na2O	0.00	0.08	0.28	0.28	0.28	0.00	0.01	0.06	0.06	0.05	0.11	0.05	0.09
K2O	8.24	8.83	8.31	8.31	8.31	9.39	8.04	8.01	7.41	8.29	5.52	3.60	7.20
Cl		0.02	0.02	0.02	0.02	0.02	0.04	0.01	0.03	0.01	0.02	0.02	0.03
F	0.00	0.18	0.37	0.37	0.37	0.18	0.34	0.74	0.22	0.29	0.30	0.09	0.76
TOTAL	93.61	95.05	95.88	95.88	95.88	95.60	94.25	95.12	91.42	96.41	92.41	89.93	94.11
Mol. prop	8O	8 O	8 O	8 O	8 O	4 O	4 O	4 O	4 O	4 O	4 O	4 O	4 O
SiO2	1.914	1.953	1.990	1.990	1.99	0.98	0.96	0.96	0.96	0.96	0.93	0.88	0.95
TiO2	0.089	0.089	0.086	0.086	0.09	0.04	0.04	0.04	0.04	0.05	0.03	0.02	0.04
Al2O3	1.320	1.268	1.272	1.272	1.27	0.64	0.64	0.64	0.65	0.61	0.60	0.63	0.62
FeO	1.092	1.056	1.017	1.017	1.02	0.52	0.58	0.60	0.56	0.61	0.69	0.75	0.62
MnO	0.004	0.001	0.004	0.004	0.00	0.00	0.00	0.00	0.00	0.00	0.00	0.00	0.00
MgO	0.617	0.634	0.605	0.605	0.60	0.30	0.32	0.31	0.32	0.31	0.36	0.43	0.33
CaO	0.003	0.002	0.007	0.007	0.01	0.00	0.00	0.00	0.00	0.00	0.00	0.00	0.00
Na2O	0.000	0.009	0.030	0.030	0.03	0.00	0.00	0.00	0.00	0.00	0.01	0.00	0.01
K2O	0.600	0.634	0.587	0.587	0.59	0.34	0.29	0.29	0.28	0.30	0.21	0.14	0.27
Cl	0.000	0.002	0.002	0.002	0.00	0.00	0.00	0.00	0.00	0.00	0.00	0.00	0.00
F	0.000	0.032	0.065	0.065	0.07	0.02	0.03	0.07	0.02	0.03	0.03	0.01	0.07
TOTAL	5.638	5.645	5.596	5.596	5.66	2.84	2.87	2.90	2.83	2.87	2.87	2.87	2.91
SiO2	0.16	0.16	0.17	0.17	0.17	0.17	0.16	0.16	0.15	0.16	0.15	0.13	0.15
TiO2	0.01	0.01	0.01	0.01	0.01	0.01	0.01	0.01	0.01	0.01	0.01	0.01	0.01
Al2O3	0.07	0.07	0.07	0.07	0.07	0.07	0.07	0.07	0.06	0.06	0.06	0.06	0.06
FeO	0.21	0.21	0.20	0.20	0.20	0.20	0.22	0.23	0.21	0.24	0.26	0.27	0.23
MnO	0.00	0.00	0.00	0.00	0.00	0.00	0.00	0.00	0.00	0.00	0.00	0.00	0.00
MgO	0.03	0.03	0.03	0.03	0.03	0.03	0.03	0.03	0.03	0.03	0.03	0.04	0.03
CaO	0.00	0.00	0.00	0.00	0.00	0.00	0.00	0.00	0.00	0.00	0.00	0.00	0.00
Na2O	0.00	0.00	0.00	0.00	0.00	0.00	0.00	0.00	0.00	0.00	0.00	0.00	0.00
K2O	0.13	0.14	0.13	0.13	0.13	0.14	0.12	0.12	0.11	0.13	0.08	0.06	0.11
Cl		0.00	0.00	0.00	0.00	0.00	0.00	0.00	0.00	0.00	0.00	0.00	0.00
F	0.00	0.00	0.01	0.01	0.01	0.00	0.01	0.02	0.00	0.01	0.01	0.00	0.02

BIOTITE CHEMISTRY										
Location	Groundrush ore zone (26005.09)					Bunkers Pit, ore zone (26005.01)				
Paragen.	Biotite (altering to or replacing chlorite) intergrown with vein quartz					Amphibole (1b.1) and biotite interlocking with granoblastic quartz in high-grade metasediment.				
weight%	9.2a	9.2b	9.2c	9.2d	9.2e	1b.1	1b.1a	1b.1b	1b.1c	1b.1d
SiO2	35.75	35.75	36.05	36.60	35.34	52.73	36.86	42.25	35.13	33.41
TiO2	1.77	1.94	2.22	2.09	1.95	0.00	1.61	0.09	1.51	1.39
Al2O3	14.63	15.78	15.78	15.43	15.30	0.42	17.78	17.73	16.85	16.43
FeO	25.36	24.16	24.09	22.60	23.55	35.12	28.73	22.86	25.79	28.50
MnO	0.21	0.19	0.20	0.22	0.18	0.24	0.12	0.08	0.05	0.05
MgO	8.41	8.38	8.17	8.29	8.27	9.35	7.42	3.40	5.89	6.61
CaO	0.01	0.00	0.02	0.05	0.00	0.29	0.27	11.04	0.18	0.04
Na2O	0.05	0.07	0.03	0.04	0.04	0.07	0.20	1.30	0.12	0.12
K2O	8.72	8.87	9.00	8.79	8.87	0.00	6.05	0.38	6.88	7.41
Cl	0.03	0.01	0.03	0.05	0.03	0.03	0.08	0.03	0.05	0.07
F	0.27	0.53	0.00	0.20	0.00	0.23	0.81	0.26	0.37	0.43
TOTAL	95.22	95.68	95.59	94.36	93.53	98.49	99.94	99.42	92.83	94.46
Mol. prop	4 O	4 O	4 O	4 O	4 O	4 O	4 O	4 O	4 O	4 O
SiO2	1.02	1.02	1.02	1.04	1.02	1.41	1.00	1.10	1.02	0.98
TiO2	0.04	0.04	0.05	0.04	0.04	0.00	0.03	0.00	0.03	0.03
Al2O3	0.49	0.53	0.53	0.52	0.52	0.01	0.57	0.54	0.58	0.57
FeO	0.61	0.57	0.57	0.54	0.57	0.78	0.65	0.50	0.63	0.70
MnO	0.01	0.00	0.00	0.01	0.00	0.01	0.00	0.00	0.00	0.00
MgO	0.36	0.35	0.34	0.35	0.36	0.37	0.30	0.13	0.26	0.29
CaO	0.00	0.00	0.00	0.00	0.00	0.01	0.01	0.31	0.01	0.00
Na2O	0.00	0.00	0.00	0.00	0.00	0.00	0.01	0.07	0.01	0.01
K2O	0.32	0.32	0.32	0.32	0.33	0.00	0.21	0.01	0.26	0.28
Cl	0.00	0.00	0.00	0.00	0.00	0.00	0.00	0.00	0.00	0.00
F	0.02	0.05	0.00	0.02	0.00	0.02	0.07	0.02	0.03	0.04
TOTAL	2.88	2.89	2.84	2.84	2.84	2.61	2.86	2.69	2.82	2.89
SiO2	0.17	0.17	0.17	0.17	0.17	0.25	0.17	0.20	0.17	0.16
TiO2	0.01	0.01	0.01	0.01	0.01	0.00	0.01	0.00	0.01	0.01
Al2O3	0.05	0.05	0.05	0.05	0.05	0.00	0.06	0.06	0.06	0.06
FeO	0.23	0.22	0.22	0.21	0.22	0.32	0.26	0.21	0.24	0.26
MnO	0.00	0.00	0.00	0.00	0.00	0.00	0.00	0.00	0.00	0.00
MgO	0.03	0.03	0.03	0.03	0.03	0.04	0.03	0.01	0.02	0.03
CaO	0.00	0.00	0.00	0.00	0.00	0.00	0.00	0.09	0.00	0.00
Na2O	0.00	0.00	0.00	0.00	0.00	0.00	0.00	0.02	0.00	0.00
K2O	0.13	0.14	0.14	0.13	0.14	0.00	0.09	0.01	0.11	0.11
Cl	0.00	0.00	0.00	0.00	0.00	0.00	0.00	0.00	0.00	0.00
F	0.01	0.01	0.00	0.00	0.00	0.01	0.02	0.01	0.01	0.01

BIOTITE CHEMISTRY

Location	Old Pirate (26023.01), OPRC076E		
Paragenesis	Metamorphic biotite in metamorphosed vein		
Wt % oxide	23-1b2	23-1b3	23-1a4
SiO2	35.29	29.44	35.72
TiO2	1.57	0.59	1.68
Al2O3	16.94	17.61	16.75
FeO	24.22	27.61	21.75
MnO	0.12	0.16	0.22
MgO	8.21	10.22	7.83
CaO	0.02	0.02	0.00
Na2O	0.00	0.01	0.01
K2O	8.09	1.84	8.99
Cl	0.04	0.02	0.03
F	0.79	0.55	0.82
Total	95.28	88.07	93.80
Mol. Prop.	6 o	6 o	6 o
SiO2	1.506	1.353	1.538
TiO2	0.050	0.020	0.054
Al2O3	0.851	0.954	0.850
FeO	0.864	1.061	0.783
MnO	0.005	0.006	0.008
MgO	0.522	0.699	0.502
CaO	0.001	0.001	0.000
Na2O	0.000	0.001	0.001
K2O	0.440	0.108	0.493
Cl	0.003	0.001	0.002
F	0.106	0.080	0.111
Total	4.347	4.286	4.343
Det. Limit.			
SiO2	0.17	0.14	0.17
TiO2	0.01	0.00	0.01
Al2O3	0.06	0.06	0.06
FeO	0.23	0.26	0.20
MnO	0.00	0.00	0.00
MgO	0.03	0.04	0.03
CaO	0.00	0.00	0.00
Na2O	0.00	0.00	0.00
K2O	0.12	0.03	0.14
Cl	0.00	0.00	0.00
F	0.02	0.01	0.02

APPENDIX FOUR:

MICROPROBE WORKSHEETS

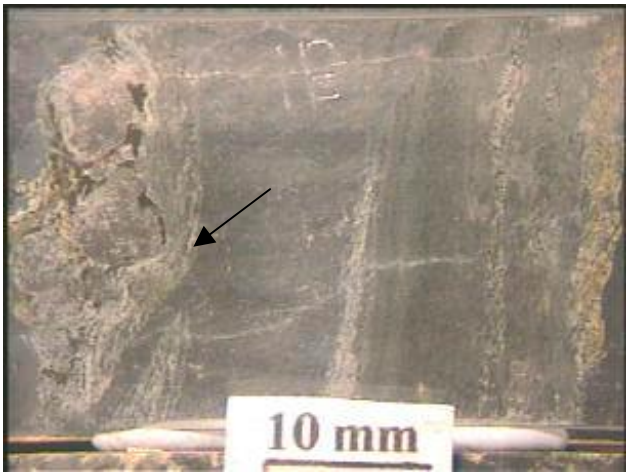

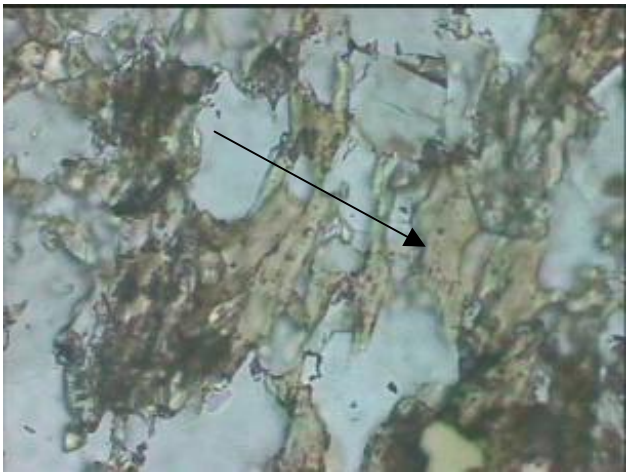

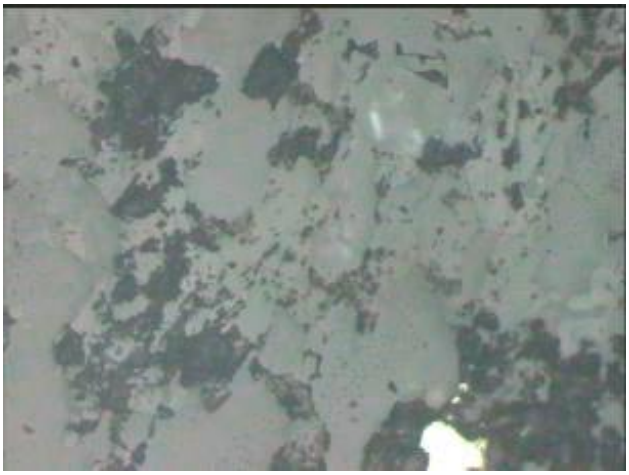

26005.01b, Bunkers Pit, Ore zone.
Biotite and amphibole (actinolite) interlocking with granoblastic quartz. Grains of pyrrhotite are present.

Biotite grains containing a maximum of 0.81 wt% F, and an average of 0.46 wt% F.
Amphibole (no Al) containing 0.23 wt% F.

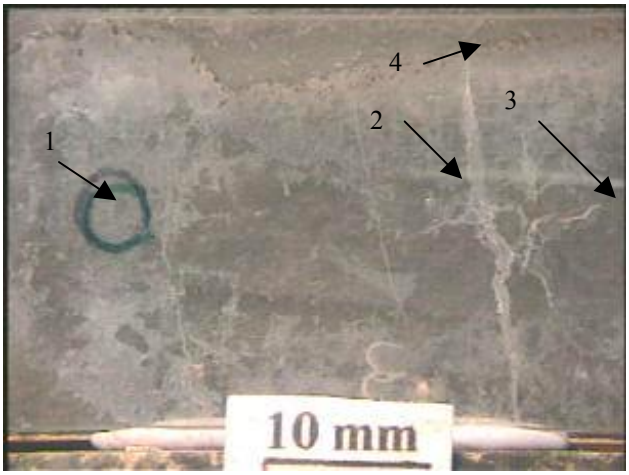

26005.03. Callie ore zone. Mineralised quartz + alkali feldspar + biotite + muscovite vein hosted by Magpie "Schist" lithology.

3.1.Galena inclusions within K-feldspar intergrown with quartz and pyrrhotite. 300 µm. rl/ppl
Galena contains up to 0.29 % Bi.

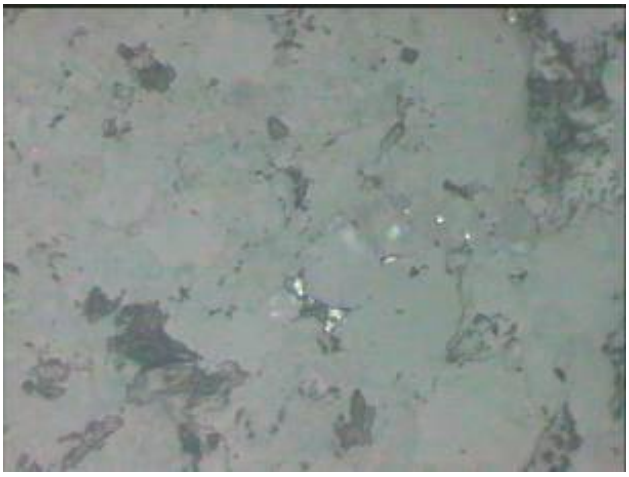

3.2. Galena interstitial to quartz and biotite. 300 µm.
Galena contains 0.28 to 0.47 wt% Bi

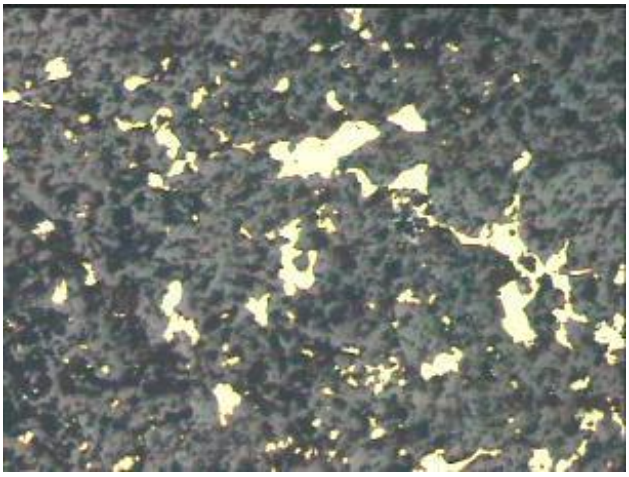

3.3. Gold intergrown with K-feldspar. 1200 µm.
Ag content: 8.46-8.78wt%
Bi content: 0.45-0.64, mean = 0.54 wt%

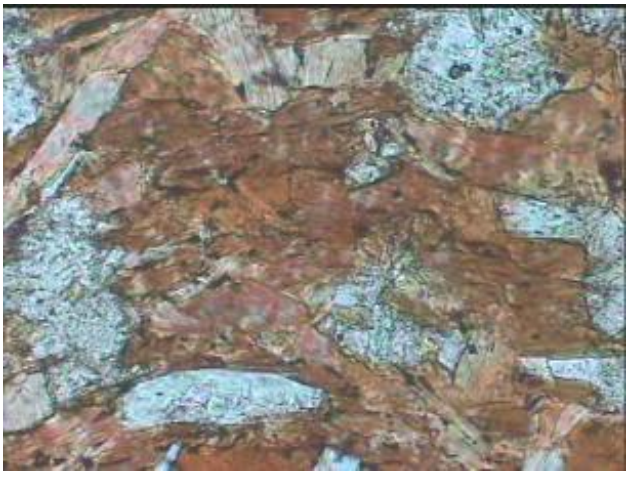

3.4. Biotite intergrown with vein quartz. 300 µm. ppl
Totals: 91-95 %. K content: 8.01 to 8.31 wt%
F content: 0.18-0.74 wt%, mean = 0.40wt %

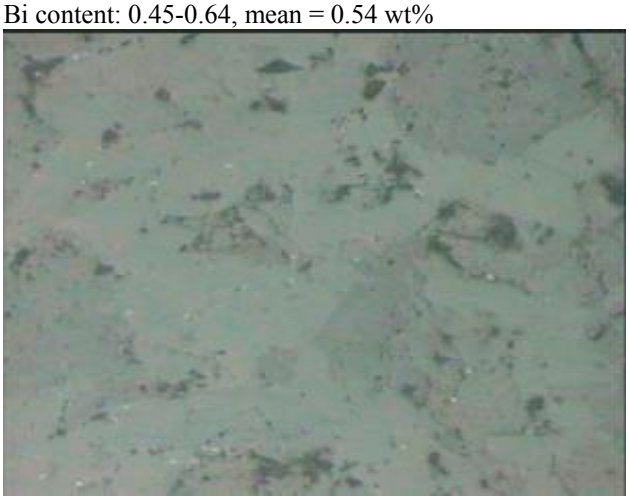

3.4. Biotite intergrown with vein quartz. 300 µm. rl

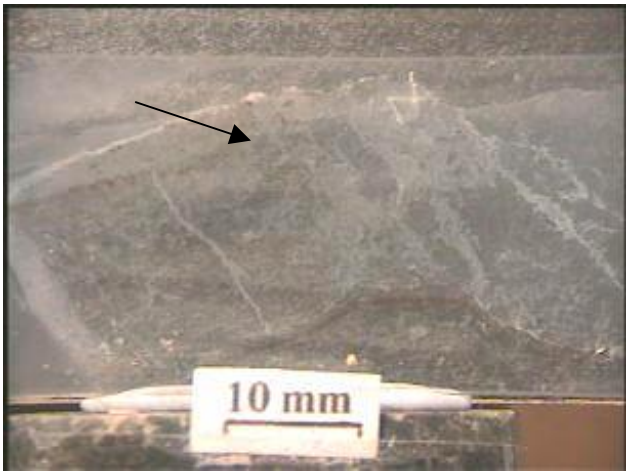

26005.04. Callie ore zone. Quartz + alkali feldspar + biotite vein hosted by Magpie schist.

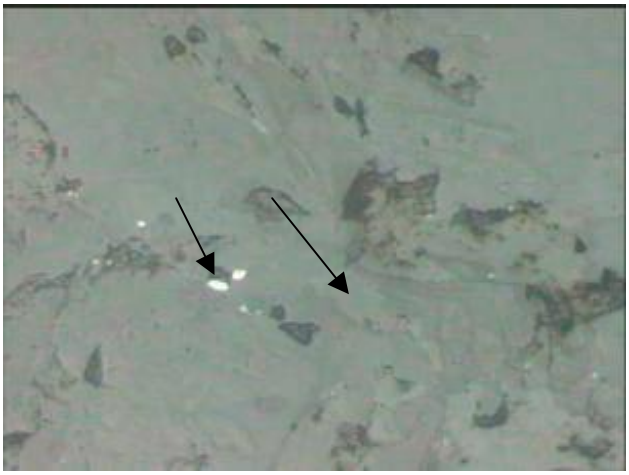

4.1. Galena intergrown with biotite and quartz. 300µm. Galena contains 0.18% Bi.

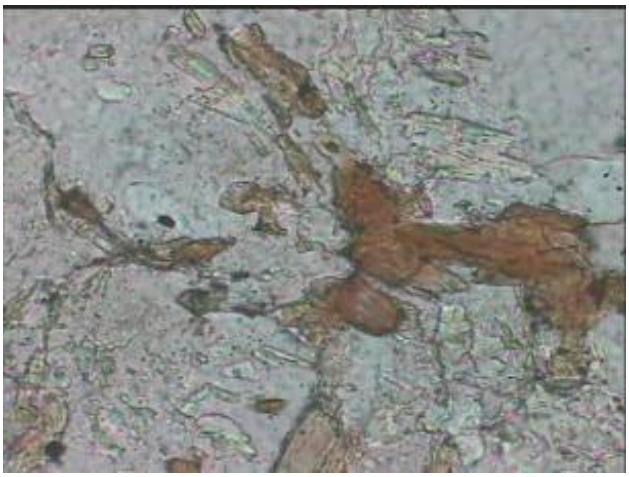

4.1. Biotite intergrown with quartz and enclosing grains of galena. 300µm. ppl

K content of biotite : 7.2-8.29wt%
Bi content of biotite: 0.29-0.76 wt% Bi, mean = 0.52 wt%

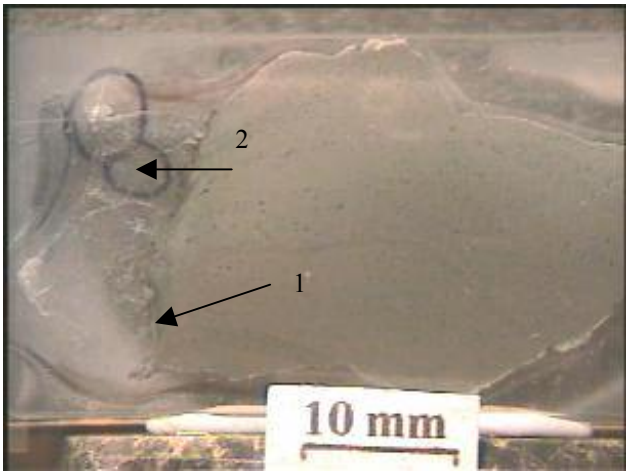

26005.06. Callie ore zone. Quartz + biotite vein hosted by "Lower Blake" beds.

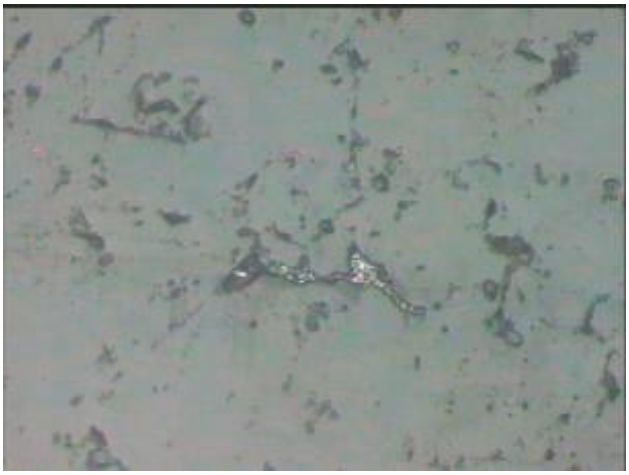

6.2. Galena interstitial to quartz. 300 μm. rl
Galena contains 0.68 wt% Bi

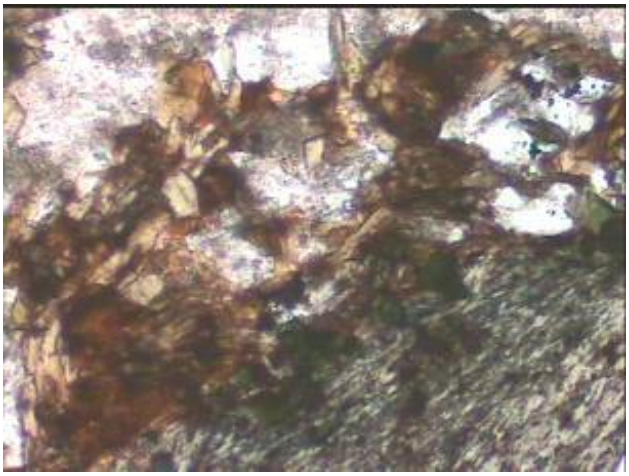

6.1.Biotite, enclosing gold, intergrown with quartz and alkali feldspar. 300 μm. ppl
Biotite totals: 93, 95, 95
K content of biotite: 8.85, 8.31, 8.31
F content of biotite: 0.18, 0.37, 0.37, mean =0.30wt%

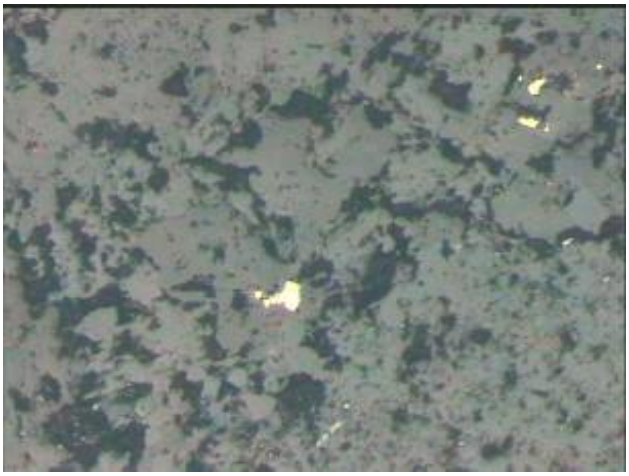

6.1. Gold intergrown with biotite, quartz and alkali feldspar. 300 μm. rl
Gold content.
Ag: 6.54, 7.27, 6.43 wt%
Bi: 0.53, 0.58, 0.71 wt%, mean = 0.60 wt%

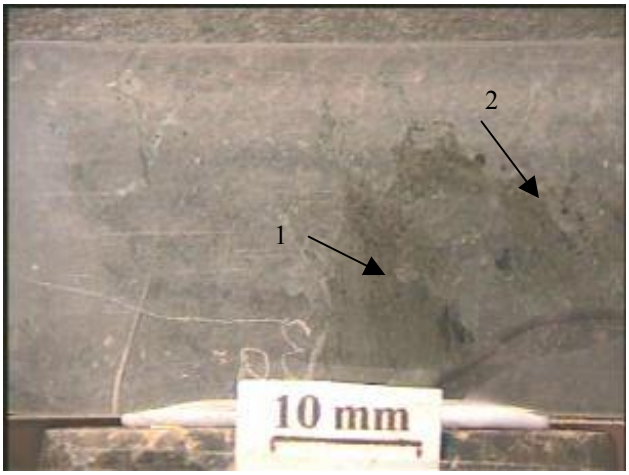

26005.09a.Groundrush ore zone. Quartz + alkali feldspar + amphibole + biotite + carbonate + chlorite vein hosted by fractured meta dolerite.

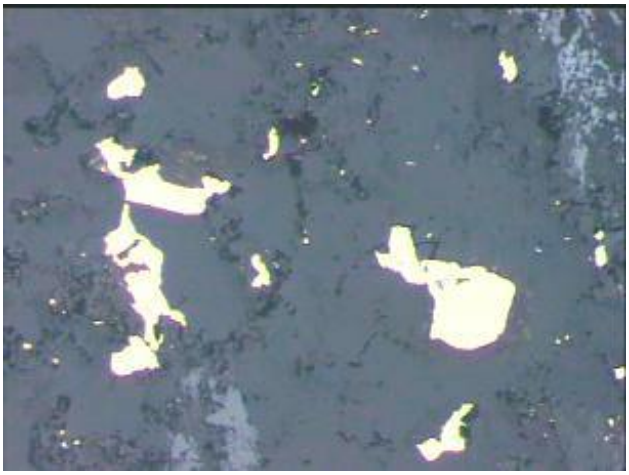

09a.1. Gold intergrown with K-feldspar, biotite and quartz after marginal wallrock fragment. 600 μm. rl.
Ag content: 6.5, 6.4, 7.0, 6.16, 6.46
Bi content: 0.54, 0.97, 0.59, 0.60, 0.67 wt%, mean =0.67wt%

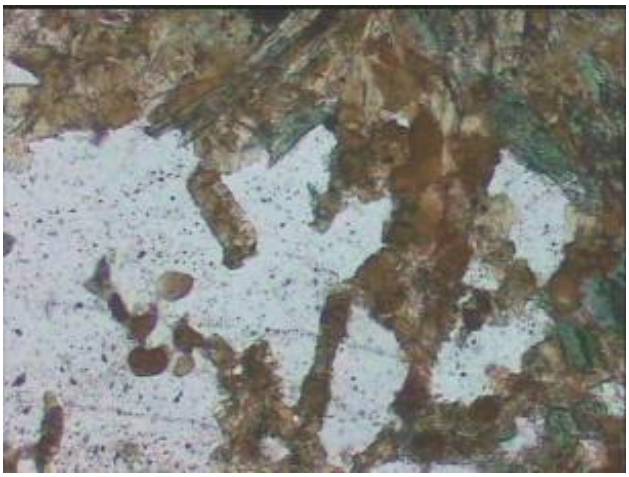

09a.2. Biotite (part altered to chlorite) intergrown with vein quartz. 600 μm.
Biotite totals: 95, 95, 95, 94, 93
F content: 0.27, 0.53, 0.11, 0.20, 0.00
K content: 8.72, 8.87, 9.00, 8.79, 8.87

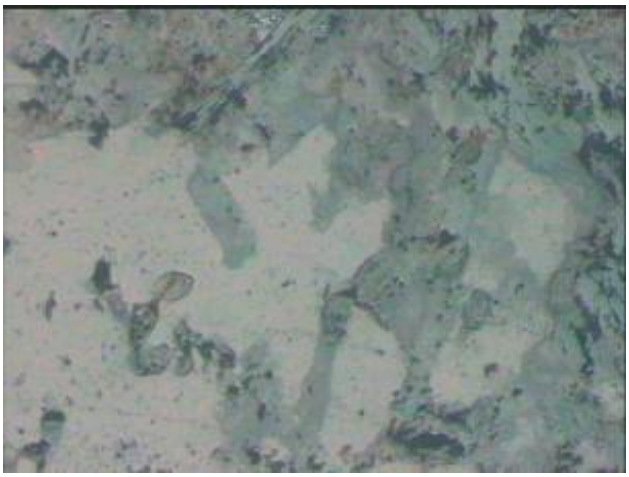

09a.2. Biotite intergrown with vein quartz. 600 μm rl

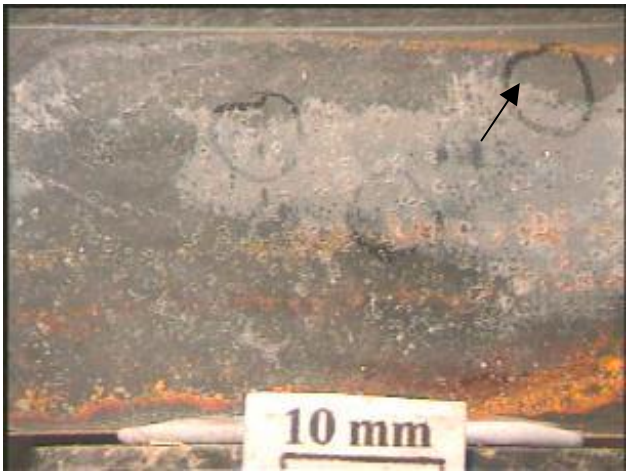

26005.07. Windy Hill ore zone. Granoblastic textured quartz veining.

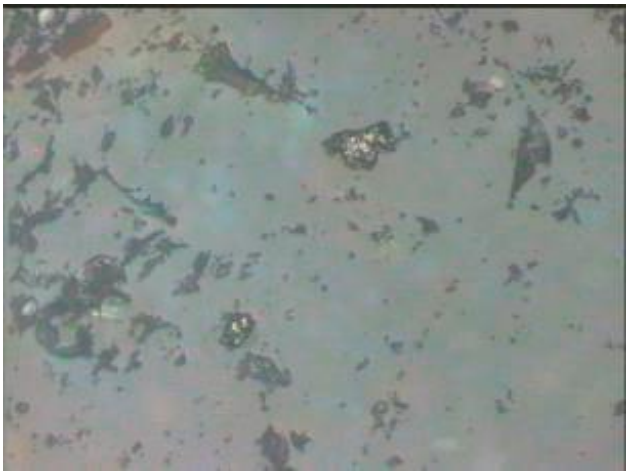

7.1. Opaque mineral as inclusions in quartz. 300 μm
Fe bearing mineral, possibly W bearing.
S present plus minor amounts of Cu.

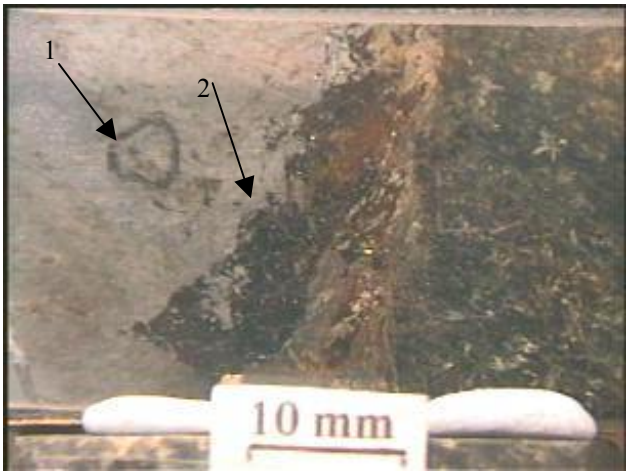

DBD352/197.8. Dead Bullock Soak ore zone quartz vein.

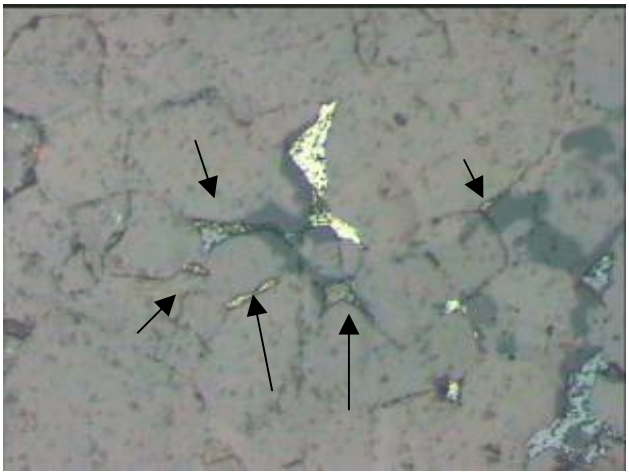

DBS.1.Sulphide minerals interstitial to granoblastic textured quartz. Recrystallisation of quartz and ductile deformation/recrystallisation of sulphides.
Pyrite, Galena, sphalerite

DBS.2.Gold intergrown with quartz and biotite (→ chlorite). 600 μm. rl
Ag content: 14.23, 13.72 wt%
Bi content: 0.8, 0.73 wt%, mean = 0.76 wt%

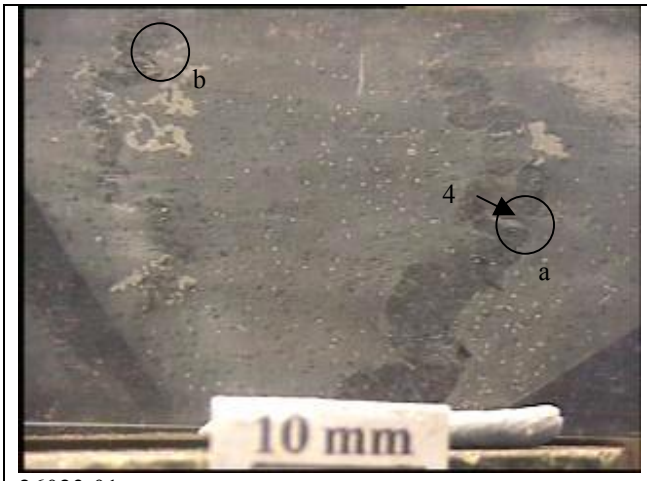

26023.01
a. 4. Biotite (0.82 wt% F).

a. (120 µm). 2. Gold (3.15 wt% Ag, 1.04 wt% Bi). 3. Gold intergrown with galena, hosted by quartz.

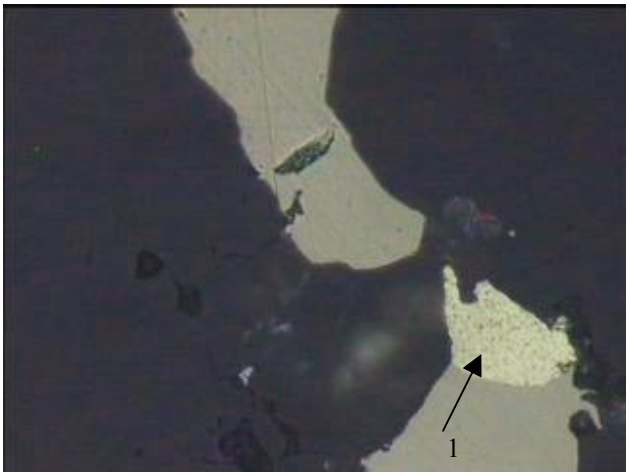

a. (120 µm). 1. Gold (11.51 wt% Ag, 0.8 wt% Bi, 0.28 wt% Cu). Intergrown with chalcopyrite and quartz.

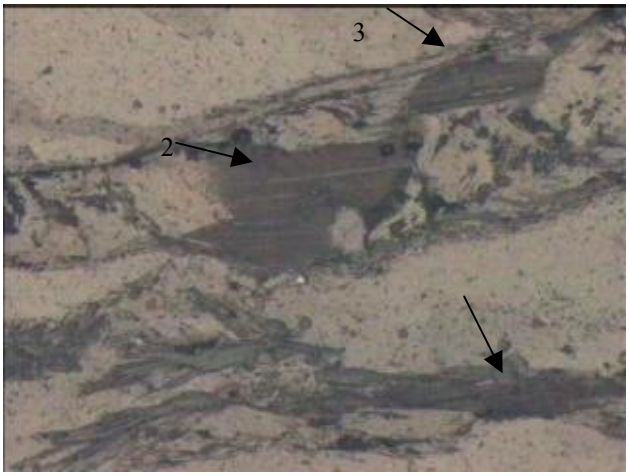

b. (600µm) 2. Biotite (0.79 wt% F). 3. Biotite (0.55 wt% F)

b. (300 µm) 1. Electrum (17 wt% Ag, 0.87 wt% Bi)

26023.01. Old Pirate. Crenulated, thermally metamorphosed quartz + carbonate + mica veins.

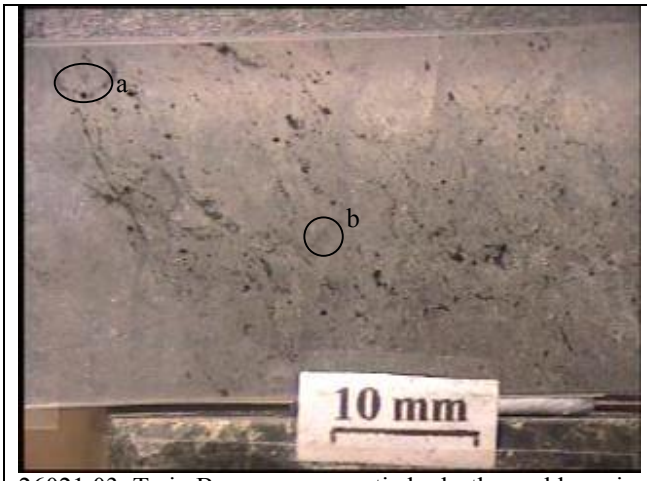

26021.03. Twin Bonanza, magnetic hydrothermal breccia

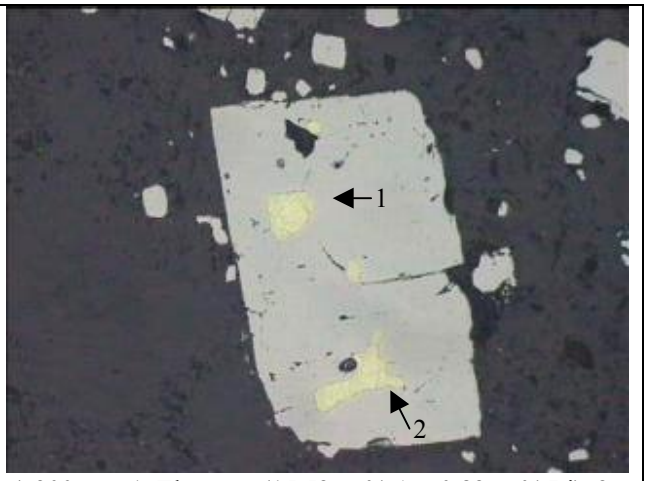

a).300 μm. 1. Electrum (15.52 wt% Ag, 0.82 wt% Bi), 2. Electrum (14.99 wt% Ag, 0.68 wt% Bi). Hosted by arsenopyrite

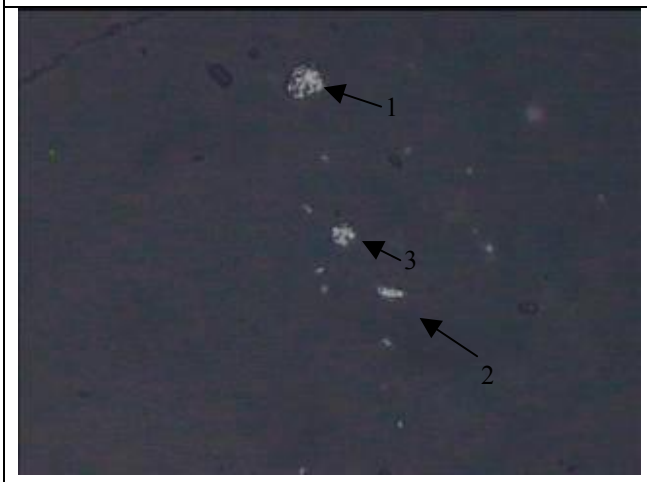

b). 120 μm. 1. Galena. 2. Acicular Boulangerite ($5PbS.2Sb_2S_3$). 3. Galena.

26020.22. Twin Bonanza, Quartz + sulphide + carbonate + K-feldspar veined granitoid porphyry.

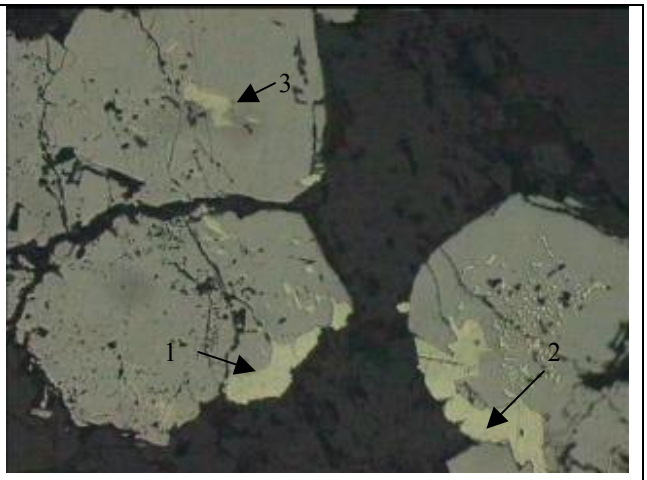

600 μm. 1. electrum (19.58 wt% Ag, 0.52 wt% Bi). 2. Electrum (21.38 wt% Ag, 0.64 wt% Bi). 3. Gold bearing galena (2.36 wt% Ag).